



**Nickolas Gueller Rocha**

**Optimization of Battery Swapping Stations  
with Battery Heterogeneity, Charging  
Degradation and PV-Option**

**Dissertação de Mestrado**

Dissertation presented to the Programa de Pós-graduação em Engenharia de Produção, do Departamento de Engenharia Industrial da PUC-Rio in partial fulfillment of the requirements for the degree of Mestre em Engenharia de Produção.

Advisor : Prof. Rafael Martinelli Pinto  
Co-advisor: Prof. Bruno Fânzeres dos Santos

Rio de Janeiro  
February 2023



**Nickolas Gueller Rocha**

**Optimization of Battery Swapping Stations  
with Battery Heterogeneity, Charging  
Degradation and PV-Option**

Dissertation presented to the Programa de Pós-graduação em Engenharia de Produção da PUC-Rio in partial fulfillment of the requirements for the degree of Mestre em Engenharia de Produção. Approved by the Examination Committee:

**Prof. Rafael Martinelli Pinto**

Advisor

Departamento de Engenharia Industrial – PUC-Rio

**Prof. Bruno Fânzeres dos Santos**

Co-advisor

Departamento de Engenharia Industrial – PUC-Rio

**Prof. Silvio Hamacher**

Departamento de Engenharia Industrial – PUC-Rio

**Prof. Rodrigo Flora Calili**

Programa de Pós-Graduação em Metrologia – PUC-Rio

**Prof. Walton Pereira Coutinho**

UFPE

Rio de Janeiro, February 15th, 2023

All rights reserved.

### Nickolas Gueller Rocha

Nickolas Gueller obtained his undergraduate degree in Industrial Engineering at PUC-rio in 2021, same university where joined the Master degree program by 2022 year also in Industrial Engineering, with emphasis in Operations Research. Nickolas also works at PSR Energy Consulting since 2021, mainly at transmission and distribution systems planning.

#### Bibliographic data

Rocha, Nickolas Gueller

Optimization of Battery Swapping Stations with Battery Heterogeneity, Charging Degradation and PV-Option / Nickolas Gueller Rocha; advisor: Rafael Martinelli Pinto; co-advisor: Bruno Fânzeres dos Santos. – 2023.

63 f: il. color. ; 30 cm

Dissertação (mestrado) - Pontifícia Universidade Católica do Rio de Janeiro, Departamento de Engenharia Industrial, 2023.

Inclui bibliografia

1. Engenharia Industrial – Teses. 2. Estação de Troca de Bateria. 3. Veículos Elétricos. 4. Produção de Energia Fotovoltaica. 5. Programas Lineares Inteiros Mistos. 6. Recursos Energéticos Distribuídos. 7. Baterias Heterogêneas. I. Martinelli Pinto, Rafael. II. Fânzeres dos Santos, Bruno. III. Pontifícia Universidade Católica do Rio de Janeiro. Departamento de Engenharia Industrial. IV. Título.

CDD: 658.5

To my Mother and Grandmother,  
for their support and guidance.

## Acknowledgments

To my Mother, for being my fundamental pillar and greatest enabler of everything that I achieved.

To my advisors Prof. Rafael Martinelli and Prof. Bruno Fânzeres, for their guidance, patience and collaboration to carry out this work.

To my work colleges of PSR, especially to João Vilela, Bruno Bernhardt and the Transmission and Distribution team, which also supported this work.

To CNPq and PUC-Rio, for the aids granted, without which this work does not could have been accomplished.

This study was financed in part by the Coordenação de Aperfeiçoamento de Pessoal de Nível Superior - Brasil (CAPES) - Finance Code 001.

## Abstract

Rocha, Nickolas Gueller; Martinelli Pinto, Rafael (Advisor); Fânzeres dos Santos, Bruno (Co-Advisor). **Optimization of Battery Swapping Stations with Battery Heterogeneity, Charging Degradation and PV-Option**. Rio de Janeiro, 2023. 63p. Dissertação de Mestrado – Departamento de Engenharia Industrial, Pontifícia Universidade Católica do Rio de Janeiro.

Greenhouse gas emissions-related issues have been extensively discussed in the past years, with over 70 countries already committed to a carbon-neutral economy by 2050. The electrification of transportation modals has increased following these goals, where Electric Vehicles (EVs) are starting to take Internal Combustion Engine Vehicles (ICEV) market share all over the globe. Besides the particular complexity in comparing EVs and ICEVs, challenges involving the nature of EVs and their integration with cities, such as the lack of public locals for charging, are also critical and interfere with their development. In this context, this work aims at studying the problem of a Battery Swapping Station (BSS), a structure where the EVs users swap their depleted batteries for fully or partially charged ones. In order to simulate the BSS daily operations and batteries charging schedule, a novel Mixed Integer Linear Programming (MILP) model is proposed, taking into account battery heterogeneity, the use of local photovoltaic (PV) production and battery degradation based on charging profile. A collection of BSS operation metrics are designed to evaluate the solution quality of the proposed scheduling model. A numerical experiment comprising four case studies based on real data from the US power and transportation systems is presented, with insights and analyses on the PV and grid power use, as well as a BSS financial comparison against close-related benchmark scheduling approaches, together with sensitivities on BSS sizing plan and costumers attendance.

## Keywords

Battery Swapping Station; Electric Vehicles; Photovoltaic Power Production; Mixed-Integer Linear Programs; Distributed Energy Sources; Battery Heterogeneity.

## Resumo

Rocha, Nickolas Gueller; Martinelli Pinto, Rafael; Fânzeres dos Santos, Bruno. **Otimização de Estações de Troca de Bateria com Baterias Heterogêneas, Degradação na Carga e Opção Fotovoltaica.** Rio de Janeiro, 2023. 63p. Dissertação de Mestrado – Departamento de Engenharia Industrial, Pontifícia Universidade Católica do Rio de Janeiro.

Problemas de emissão de gases de efeito estufa vem sido amplamente discutidos nos últimos anos, uma vez que mais de 70 países já se comprometeram a uma economia neutra em carbono até 2050. A eletrificação dos modais de transporte tem sido ampliadas seguindo essas metas, onde os Veículos Elétricos (VEs) começam a ganhar participação sobre o mercado de Veículos com Motor de Combustão Interna (VMCI) por todo o mundo. Além da particular complexidade na comparação entre VEs e VMCI, desafios envolvendo a natureza dos VEs e sua integração com as cidades, como a falta de locais públicos para recarga, também são críticos e interferem no seu desenvolvimento. Nesse contexto, este trabalho visa estudar o problema de uma Estação de Troca de Baterias (ETB), uma estrutura onde os usuários de VEs trocam suas baterias descarregadas por outras totalmente ou parcialmente carregadas. No intuito de simular as operações diárias do ETB e o cronograma de carregamento das baterias, um novo modelo de Programação Linear Inteira Mista (PLIM) é proposto, levando em consideração a heterogeneidade da bateria, o uso de geração fotovoltaica (PV) local e a degradação da bateria com base no perfil de carregamento. Uma coleção de métricas de operação do ETB é projetada para avaliar a qualidade da solução do modelo de cronograma proposto. É apresentado um experimento numérico que compreende quatro estudos de caso baseados em dados reais dos sistemas de energia e transporte dos EUA, contendo insights e análises sobre o uso da energia fotovoltaica e da rede, bem como uma comparação financeira do ETB com abordagens de cronograma de benchmarks relacionados, juntamente de sensibilidades no plano de dimensionamento do ETB e atendimento a clientes.

## Palavras-chave

Estação de Troca de Bateria; Veículos Elétricos; Produção de Energia Fotovoltaica; Programas Lineares Inteiros Mistos; Recursos Energéticos Distribuídos; Baterias Heterogêneas.

## Table of contents

<b>1</b>	<b>Introduction</b>	<b>12</b>
1.1	Objectives and Contributions Regarding the Existing Literature	14
<b>2</b>	<b>Battery Swapping Station and Business Model</b>	<b>16</b>
<b>3</b>	<b>BSS Operational Scheduling Formulation</b>	<b>18</b>
3.1	Formulation	19
<b>4</b>	<b>Case Study</b>	<b>30</b>
4.1	Data Setup	30
4.2	Cases Description	36
4.3	BSS Metrics	37
<b>5</b>	<b>Numerical Experiments</b>	<b>40</b>
5.1	Case Studies Overview	40
5.2	Model Extensions Evaluation	43
5.3	Case 1 Analyses	47
<b>6</b>	<b>Conclusion</b>	<b>59</b>



## List of figures

Figure 2.1	Battery Swapping Station System	17
Figure 3.1	Battery degradation curve linearized for 15min time slots	26
Figure 3.2	Charging Power (Basic)	28
Figure 3.3	Charging Power (C-Control)	28
Figure 4.1	USA Hourly Urban Interstates Traffic Distribution	31
Figure 4.2	PV Power Distribution	33
Figure 4.3	PV Generation Distribution in 15 min horizon	34
Figure 4.4	Average Hourly Real Time Energy Price by AECO zone in 2019	36
Figure 5.1	Case Studies Profit Overview	41
Figure 5.2	Case Studies Metrics Overview	42
Figure 5.3	Profit Comparison for Case 1	43
Figure 5.4	Metrics Comparison for Case 1	43
Figure 5.5	Profit Comparison for Case 2	44
Figure 5.6	Metrics Comparison for Case 2	44
Figure 5.7	Profit Comparison for Case 3	44
Figure 5.8	Metrics Comparison for Case 3	45
Figure 5.9	Profit Comparison for Case 4	45
Figure 5.10	Metrics Comparison for Case 4	45
Figure 5.11	Charging schedule for $m = 1, b = 2$	47
Figure 5.12	Charging schedule for $m = 2, b = 3$	48
Figure 5.13	PV Energy use and Energy Price	49
Figure 5.14	PV Use and Energy Price	50
Figure 5.15	PV Energy use and Energy Price	51
Figure 5.16	EV Energy Attendance for Model 1	52
Figure 5.17	EV Energy Attendance for Model 2	53
Figure 5.18	BSS Evaluation for Model 1	54
Figure 5.19	BSS Evaluation for Model 2	54
Figure 5.20	BSS Profit and Metrics Relation with Batteries Number	56
Figure 5.21	BSS Profit and Metrics Relation with PV Capacity	57
Figure 5.22	BSS Profit and Degradation relation with Service Level	58

## List of tables

Table 3.1	Battery Degradation Adaptation	25
Table 4.1	BSS General Configuration	30
Table 4.2	BSS Batteries Configuration	35
Table 4.3	Study Cases Description Summary	37
Table 4.4	Cases Instances Arrivals Summary	37
Table 5.1	Case studies results	41
Table 5.2	Case studies average results	41
Table 5.3	BSS Economical Evaluation	55



# 1

## Introduction

During the past years problems induced by large emission levels of Greenhouse Gases (GHGs) have been widely discussed around the globe. Several countries have already committed to net zero carbon emissions by 2050 [1], inducing the development of multiple techniques to trade, plan, control, and operate power systems with large levels of renewable penetration [2, 3, 4]. In this context, the electrification of transportation modals has gained momentum following these net-zero goals, leading to Electric Vehicles (EVs) to increase their market share all over the world. In fact, despite the pandemic-related worldwide downturn in car sales, with an estimated global overall drop of 16%, electric car registrations increased by 41% in 2020 [5]. Although the increasing penetration of EV and their benefits to air pollution and citizens health [6], there are still critical aspects that current EV systems and related infrastructure are not capable of efficiently handle in comparison to Internal Combustion Engine Vehicles (ICEVs). One can cite for their driving range and time spent in the battery charging process.

Furthermore, the lack of public locals for charging and stations, electric network distribution congestion, battery degradation and recycling process are also critical for a sustainable integration of EVs in modern cities. On the one hand, charging stations, also named Battery Charging Station (BCS), are the most popular adaptation of the current gas stations for the EVs. This type of structure requires hours of wait until the EV replenishes their batteries, which induces loss of time and higher costs for commercial applications. Although it is possible to make use of fast chargers to decrease the charging time, the process increases the battery degradation effect, reducing battery lifetime as a consequence<sup>1</sup> [8]. The installation of EV chargers at public or private parking lots, on the other hand, would expand the access to charging locals, where EV owners would take advantage of the parked car time, enabling even an overnight recharging. However, it is not always a feasible solution due to network congestion and other aspects.

In this context, an alternative solution would be to use the so-called Battery Swapping Station (BSS), a structure where the EVs would only swap their depleted batteries for fully or partially charged ones. While the EVs would need hours to fully charge their batteries in a BCS, the BSS can provide

<sup>1</sup>A complete discussion and analyses of the key challenges involving fast charging infrastructure can be found in [7]

a swapping service in few minutes (e.g., less than 5 minutes) [9], thus being recognized as a more viable solution than the standard BCS [10]. Recently, Tesla<sup>®</sup> presented a battery swapping simulation for its Model S, where the charging procedure was even faster than refill a gas tank. In addition, a commercial use of BSS was made in China during the 2008 Summer Olympics for electric buses [11]. Moreover, lining up with the desired net-zero emission target, BSS can be operated with Photovoltaic (PV) panels such as a recent application in Germany [12]. From an electrical-grid-wide perspective, several benefits in promoting the battery swapping process are pointed in [13], with the main ones being the load peak shaving, by the grid operator perspective, and costumers benefits with EV price reduction by the adoption of battery leasing business model, keeping the ownership for the BSS or some company. Since battery costs by itself can account for up to one-third of total EV costs [14], the leasing model can promote higher EV accessibility.

Although the BSS adoption can provide multiples benefits, several operational challenges still need to be addressed, such as the batteries charging schedule, demand forecast and battery lifetime management. In [9], a wide discussion over battery degradation, interchangeability, and feasibility is presented. Furthermore, a wide range of BSS studies involving mathematical models and Monte Carlo Simulation [15], BSS integration with power grid [16] and the BSS economic advantages translated into a business case [17] can be found in technical literature. In this sense, the use of computational models can bring insights about the BSS daily operation and all trade-offs decisions involved, especially in cases with hundreds of batteries, different battery models, subjected to hundreds of EV arrivals at a day.

Given the BSS context challenges and based on the developed research of [18], in this work, we propose a mathematical model that represents the daily operation of a BSS considering PV generation, taking into account critical feasibility and sustainability features for the business in the long-term, such as battery heterogeneity and battery degradation due to charging process. The model's main objective is to maximize the daily profit of the BSS considering the decision of the batteries charging schedule and the acceptance/rejection of the EVs swapping requests. A collection of BSS operation metrics are also designed in this work to evaluate the solution quality of the proposed scheduling model. A numerical experiment comprising four case studies based on real data from the US power and transportation systems from 2019 is presented in order to illustrate the applicability and benefits of the proposed model in different contexts. Results highlighted the importance of battery degradation in the optimization model, since its consideration as an operational

cost brought a reduction of 16%. Moreover, the BSS developed measurement metrics enabled analyses along profitability towards the swapping process, as well as operation impact of changes in the number of batteries and PV capacity.

## 1.1

### Objectives and Contributions Regarding the Existing Literature

Several works can be found in technical literature where the BSS is discussed over different aspects. Aiming at contextualizing the contributions of this paper, some related works are discussed further on. A multi-objective optimal scheduling of a BSS considering the number of batteries taken from stock, charging damage, and charging cost has been shown in [19]. The Shuffled Frog Leaping Algorithm was used to solve the model. In [20], a mathematical model was developed to minimize the BSS operation cost considering uncertainty constraints, random customer demands of fully charged batteries, demand shifting and energy sell back. The battery degradation process was also modeled to ensure a practical solution.

Within the Microgrid (MG) perspective, [21] proposed a bi-level scheduling framework for optimal operation scheduling of MG and BSSs as two independent stakeholders with inherently conflicting objectives. Moreover, battery degradation cost was explicitly modeled and a hybrid probabilistic-possibilistic approach considering correlation among uncertainties has been developed.

Taking into account studies where the BSS used distributed generation, [22] studied an integrated PV-BSS model considering battery degradation, speed-variable charging and weather/traffic forecast, solved using Particle Swarm Optimization techniques.

The main reference study of this work is [18], which developed a mixed integer non-linear model to define PV-based BSS operations, where sensitivity analyses were made upon homogeneity of batteries. The study concluded that the PV could increase the BSS profit by 67% and decreases costumer's non-attendance. The proposed model also enables the sale of partially charged batteries, as long as the battery level stays greater or equal to the costumer minimum desired level. Moreover, in [18] it is also cited the lack of studies in the literature considering a BSS operation with renewable generation, highlighting the existing literature gap.

The referenced researches usually develop algorithms and solution methods in order to solve a BSS model, or even bring aspects such as battery degradation and uncertainty. However, there is a lack of studies that details the BSS operation with measurement metrics to bring usable insights for BSS operators. Moreover, it was not found a study that mixes the use of PV gener-

ation, battery heterogeneity (multiple battery types) and battery degradation in a BSS context.

In this sense, contextualizing usable insights, this work presents numerical experiments in cases developed based on real data from the USA power and transportation systems. Furthermore, a basic model formulation is presented based on the enhancement of the developed model by [18], where two extensions are proposed and further evaluated based on the consideration of battery degradation and a control over the batteries charging profile. To summarize, the main contributions of this work are fourfold:

1. Development of a novel mathematical model to obtain the daily schedule of a BSS considering multiple battery types, PV generation flexible use and battery degradation, extending the presented model in [18];
2. Development of a battery degradation cost model based exclusively on the batteries charging power, adapting the developed model in [23];
3. Proposal of BSS measurement metrics based on operation decisions;
4. Insights provision about the BSS daily operation and sensitivity to the station configuration such as number of batteries and PV capacity.

The remainder of the paper is organized as follows. Section 2 discusses about the BSS considered business model, while Section 3 presents the problem formulation. In Section 4 the case studies development is described and the numerical experiments are shown in Section 5. Finally, Section 6 brings the study conclusion and future works proposition.

## 2

### Battery Swapping Station and Business Model

A BSS functioning involves the use of a swapping lane, where the EVs shall have their batteries swapped in a matter of minutes, an information system responsible for all data flow such as swapping requests and charging schedule decision, and at last an internal charging station, where the EVs depleted batteries will be recharged along the day for the next swapping. A key factor for a BSS economical feasibility is the energy contract, since the decided energy price for the swapped batteries must be based on the expected energy price of the day (which varies over the hours). The ideal price should be lower than the peak price, otherwise EV costumers will prefer a BCS use, while also maintain a price value that brings considerable profit for the swapping service. A possible gain-gain zone that can be provided by the BSS would be to charge the batteries at the cheapest hours of the day and delivery the batteries at a slightly higher price during the peak price hours, still maintaining a lower price than the peak.

Furthermore, an expected challenge for a BSS operation is the uncertainty in the EVs swapping requests, since the batteries must be previously charged before their arrivals and the energy price can be extremely volatile along the day. Since the EVs market penetration is a future trend for several countries, whereby the technology will be also further developed, a reasonable assumption for the BSS context support would be the use of Internet of Things (IoT) devices, specially for the EVs swapping requests data.

Overall, advances in technology, innovation and artificial intelligence (AI) can be seen everyday with the development of new products and concepts. In this sense, by the energy sector, these advances can be seen with the development of smart grids and smart cities [24], as well as the use of Internet of Things (IoT) devices. Moreover, it is expected that the amount of data from the IoT that is analyzed and used to change business processes will be as significant in 2025 as all the data created in 2020 [24]. In this sense, AI is starting to play a major role in the energy market, including applications in electric distribution networks and energy storage systems, which can be seen in further detail in [25].

In this sense, the present research will consider a BSS system that makes use of IoT devices within its operation in order to reduce the EVs swapping requests uncertainties along the day. Such data which will be assumed as known along the day includes the EVs respective batteries model, State of Charge



(SoC)<sup>1</sup> by time of arrival at the station, as well as their State of Health (SoH)<sup>2</sup>.

The BSS operation to be considered in this study can be illustrated by Fig. 2.1. It is assumed that the EVs are constantly connected to the internet, thus constantly sending swapping requests to a BSS. The station's information system receives the EV request and specifications, estimating its energy level by the arrival time. Requests rejection due to infeasibility will redirect the EV request to another BSS. Gathering the accepted swapping requests, the information system creates a charging schedule which will be followed by the BSS, where the batteries can be charged up with grid and/or PV power. The PV power can also be fully or partially sold to the grid based on the sale price. Moreover, due to business deals with the local system operator, day-ahead energy spot prices will be assumed as known. Also, the BSS will receive a recommended upper bound for the total power charged from the grid, where there will be a price increase percentage on all power which exceeds this recommended limit.

Under the operations of automatic systems (e.g., robots), the incoming EVs get their depleted battery swapped in a few minutes with a reliable process. At last, the batteries are assumed to be belonging to the BSS, therefore all costs involving degradation and battery replacement are assumed by the station.

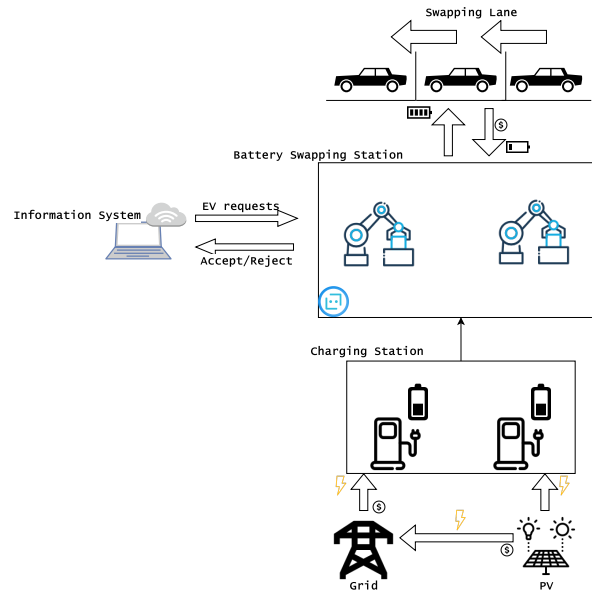


Figure 2.1: Battery Swapping Station System

<sup>1</sup>Defined as the battery actual energy level as a percentage value of its capacity

<sup>2</sup>Defined as the battery health in terms of capacity fading percentage, since the degradation process reduces its storage capacity

### 3

## BSS Operational Scheduling Formulation

The main objective of this work is to leverage mathematical programming techniques to develop a novel daily operational scheduling methodology for BSS considering multiple battery types, PV generation flexible use and battery degradation. For this purpose, the following general assumption over the business context are made:

1. PV generation is treated deterministically based on forecast values;
2. Battery pack swapping time, as well as the time between arrivals, is set to 15 min. The BSS is equipped with only one swapping mechanism per type of vehicle, therefore only one EV per type can be serviced at each period;
3. Energy losses in general are ignored;
4. There is no purchase or sale of batteries, therefore the number of batteries remains constant;
5. Day-ahead electricity price is known due to grid operator shared information;
6. Since the work focuses on measure the BSS performance upon costumer attendance, energy sellback to grid is limited by the PV generation.
7. It will be assumed that all swapping requests will be serviced, i.e, a costumer attendance of 100%, as well as that the BSS is well sized in order to make it possible;
8. Batteries are charged with a DC charger and it is assumed that EV costumers accepts partially charged batteries, as long as their minimum desired battery levels is serviced;
9. EV arrivals by BSS are assumed to be correlated with traffic volume;
10. The BSS will be available for swapping requests during 07:00AM to 10:00PM and will close at 11:00PM;
11. Battery degradation is considered based on the charging profile described by an empirical function developed in [23].

## 3.1

## Formulation

Sets and Indexes:

$\mathcal{T}$	Set of time slots with index $t$ and final stage slot $t_f$
$\mathcal{M}$	Set of battery models with index $m$
$\mathcal{B}_m$	Set of batteries number of type $m$ with index $b$

Parameters:

$\pi_t$	Energy spot price per kWh at time $t$	$\bar{E}_m$	Energy capacity of battery model $m$
$\lambda$	Price per kWh swapped	$SOC^{t_f}$	Final day minimum SOC
$N$	Number of chargers present at the BSS	$\tilde{E}_{t,m}$	Minimum allowed energy level of a battery model $m$ to attend a swapping request at time $t$
$\underline{R}_m$	Minimum power rate for battery $m$	$\bar{R}_m$	Maximum power rate for battery $m$
$D$	Time step fraction of an hour	$E_t^{PV}$	PV generation at time $t$
$E_{t,m}^{EV}$	Remaining energy level of incoming EV at time $t$ , with battery model $m$	$L$	Maximum recommended charging power limit from the grid
$A_{t,m}$	Binary matrix of EV arrivals at time $t$ (1 if has an arrival of model $m$ , 0 otherwise)	$\delta^+$	Cost percentage increase for exceeding power of the recommended limit

Decision Variables:

$E_{t,m,b}$	Energy level of battery number $b$ , model $m$ , at time $t$	$P_{t,m,b}^T$	Total charging power destined to the batteries
$\Delta E_{t,m,b}$	Energy sold during an accepted swapping at time $t$	$SOC_{t,m,b}$	State Of Charge for each BSS battery
$P_{t,m,b}^{PV}$	Charging power provided by the PV	$E_t^{PVS}$	PV energy sold to the grid
$P_{t,m,b}^G$	Charging power provided by the grid	$K_{t,m,b}$	Battery charging status at time $t$ (1 if in charging, 0 otherwise)
$Pb_{t,m,b}$	Charging power from the grid below the recommended limit	$S_{t,m,b}$	Battery swapping status at time $t$ (1 if being swapped, 0 otherwise)
$Pa_{t,m,b}$	Charging power from the grid above the recommended limit	$E_{t,m,b}^{PV}$	Energy provided by the PV

The mathematical formulation extends the one developed in [18]. The battery charging schedule is the decision variable involved and the main goal is to maximize the BSS daily profit over the daily operations horizon, divided into time steps of 15 minutes ( $D = 1/4$ ). The daily decisions of the BSS depend mainly on aspects such as the batteries charging status, i.e., which moments the batteries will be keep in charging at a certain power rate, as well as the acceptance of EV costumers swapping requests at each period, for each type of battery. These decisions are represented by the model variables  $P_{t,m,b}^T$ ,  $K_{t,m,b}$ , and  $S_{t,m,b}$ , respectively, and they are present in most of the model constraints. Moreover, environment aspects such as the electricity price  $\pi_t$ , PV generation forecast  $E_t^{PV}$  and the remaining energy level for each arriving  $E_{t,m}^{EV}$  are considered by the model and have directly influence at the optimal batteries schedule. The proposed model is formulated as the following mixed-integer non linear programming (MINLP) problem.

$$\text{Max} \quad \sum_{t \in \mathcal{T}} \sum_{m \in \mathcal{M}} \sum_{b \in \mathcal{B}_m} \lambda \Delta E_{t,m,b} \quad (3-1)$$

$$+ \sum_{t \in \mathcal{T}} \pi_t E_t^{PVS} \quad (3-2)$$

$$- \sum_{t \in \mathcal{T}} \sum_{m \in \mathcal{M}} \sum_{b \in \mathcal{B}_m} D(\pi_t P b_{t,m,b} + (1 + \delta^+) \pi_t P a_{t,m,b}) \quad (3-3)$$

$$- \phi(K) \quad (3-4)$$

Subject to:

$$E_{t,m,b} = E_{t-1,m,b} + (DP_{t,m,b}^T) - \Delta E_{t,m,b} \quad \forall t \in \mathcal{T}, m \in \mathcal{M}, b \in \mathcal{B}_m \quad (3-5)$$

$$\Delta E_{t,m,b} = (E_{t-1,m,b} - E_{t,m}^{EV}) S_{t,m,b} \quad \forall t \in \mathcal{T}, m \in \mathcal{M}, b \in \mathcal{B}_m \quad (3-6)$$

$$K_{t,m,b} + S_{t,m,b} \leq 1 \quad \forall t \in \mathcal{T}, m \in \mathcal{M}, b \in \mathcal{B}_m \quad (3-7)$$

$$E_{t,m,b} \leq \bar{E}_m \quad \forall t \in \mathcal{T}, m \in \mathcal{M}, b \in \mathcal{B}_m \quad (3-8)$$

$$SOC_{t,m,b} = \frac{E_{t,m,b}}{\bar{E}_m} \cdot 100 \quad \forall t \in \mathcal{T}, m \in \mathcal{M}, b \in \mathcal{B}_m \quad (3-9)$$

$$SOC_{t=t_f,m,b} \geq SOC^{t_f} \quad \forall m \in \mathcal{M}, b \in \mathcal{B}_m \quad (3-10)$$

$$E_{t-1,m,b} \geq \tilde{E}_{t,m} S_{t,m,b} \quad \forall t \in \mathcal{T}, m \in \mathcal{M}, b \in \mathcal{B}_m \quad (3-11)$$

$$\sum_{b \in \mathcal{B}_m} S_{t,m,b} = A_{t,m} \quad \forall t \in \mathcal{T}, m \in \mathcal{M} \quad (3-12)$$

$$\sum_{m \in \mathcal{M}} \sum_{b \in \mathcal{B}_m} K_{t,m,b} \leq N \quad \forall t \in \mathcal{T} \quad (3-13)$$

$$\underline{R}_m K_{t,m,b} \leq P_{t,m,b}^G \leq \bar{R}_m K_{t,m,b} \quad \forall t \in \mathcal{T}, m \in \mathcal{M}, b \in \mathcal{B}_m \quad (3-14)$$

$$P_{t,m,b}^T = P_{t,m,b}^{PV} + P_{t,m,b}^G \quad \forall t \in \mathcal{T}, m \in \mathcal{M}, b \in \mathcal{B}_m \quad (3-15)$$

$$E_t^{PV} = \sum_{m \in \mathcal{M}} \sum_{b \in \mathcal{B}_m} E_{t,m,b}^{PV} + E_t^{PVS} \quad \forall t \in \mathcal{T} \quad (3-16)$$

$$P_{t,m,b}^{PV} = \frac{E_{t,m,b}^{PV}}{D} \quad \forall t \in \mathcal{T}, m \in \mathcal{M}, b \in \mathcal{B}_m \quad (3-17)$$

$$P_{t,m,b}^G = Pb_{t,m,b} + Pa_{t,m,b} \quad \forall t \in \mathcal{T}, m \in \mathcal{M}, b \in \mathcal{B}_m \quad (3-18)$$

$$\sum_{m \in \mathcal{M}} \sum_{b \in \mathcal{B}_m} Pb_{t,m,b} \leq L \quad \forall t \in \mathcal{T} \quad (3-19)$$

$$E_{t,m,b}, \Delta E_{t,m,b}, P_{t,m,b}^{PV} \geq 0 \quad \forall t \in \mathcal{T}, m \in \mathcal{M}, b \in \mathcal{B}_m \quad (3-20)$$

$$P_{t,m,b}^G, Pb_{t,m,b}, Pa_{t,m,b} \geq 0 \quad \forall t \in \mathcal{T}, m \in \mathcal{M}, b \in \mathcal{B}_m \quad (3-21)$$

$$P_{t,m,b}^T, SOC_{t,m,b} \geq 0 \quad \forall t \in \mathcal{T}, m \in \mathcal{M}, b \in \mathcal{B}_m \quad (3-22)$$

$$E_t^{PVS} \geq 0 \quad \forall t \in \mathcal{T} \quad (3-23)$$

$$S_{t,m,b}, K_{t,m,b} \in \{0, 1\} \quad \forall t \in \mathcal{T}, m \in \mathcal{M}, b \in \mathcal{B}_m \quad (3-24)$$

$$\left( K_{t,m,b}, K_{t-1,m,b}, S_{t,m,b} \right) \in \Omega \quad \forall t \in \mathcal{T}, m \in \mathcal{M}, b \in \mathcal{B}_m \quad (3-25)$$

The objective function of the proposed model is illustrated by (3-1) – (3-4). Expression (3-1) represents the swapping revenue of the BSS, which is based on the energy sale  $\Delta E_{t,m,b}$  of an accepted swapping request, evaluated at a fixed price  $\lambda$  per kWh to the costumer. Therefore, costumers only pay for the energy they receive in the swapped battery, discounting the energy of the depleted battery. Expression (3-2) represents the revenue provided by the sale of PV generation to the grid  $E_t^{PVS}$  at spot price  $\pi_t$ . Expression (3-3) represents the energy purchase costs from the grid, where  $Pb_{t,m,b}$  is the part below the recommended limit, with energy price  $\pi_t$ , and  $Pa_{t,m,b}$  is the power that exceeds

it, receiving a price increase of  $\delta^+$ %. All the related power is used during the chosen time step  $D$  given in hours. Finally, (3-4) considers the use of  $\phi(K)$  function, which describes the degradation cost and will be further explained in Section 3.1.2.

Constraints (3-5) define the energy level balance of the batteries, where the previous energy level ( $E_{t-1,m,b}$ ) is added with the charged energy ( $D \cdot P_{t,m,b}^T$ ) and balanced with the sold energy ( $\Delta E_{t,m,b}$ ), in case a swapping request is assigned to that battery. In (3-6) the energy sold to a costumer is defined, being null when the swapping request is not accepted ( $S_{t,m,b} = 0$ ), otherwise it becomes the difference to the energy level of the income EV costumer depleted battery ( $E_{t,m,b}^{EV}$ ).

Constraints (3-7) indicate a relation of mutual exclusion between the charging status ( $K_{t,m,b}$ ) and the swapping acceptance ( $S_{t,m,b}$ ), establishing that a battery can be either swapped or charged or neither swapped nor charged. On the other hand, Constraints (3-8) bound the battery energy level with the respective model capacity ( $\bar{E}_m$ ).

Equations (3-9) define the batteries State of Charge (SoC), while (3-10) establish the batteries minimum SoC in the final time slot, that way all batteries will start the next day at the desired level ( $SOC^{tf}$ ). Constraints (3-11) establish that a swap request can only be accepted if the battery satisfies the minimum desired energy level ( $\tilde{E}_{t,m}$ ) of the respective costumer. Constraints (3-12) establish the swapping attendance based on the binary matrix  $A_{t,m}$ , which is equal to one if there is an EV arrival of model  $m$  at time  $t$  and zero otherwise. Moreover, as long as there is an EV arrival, only one swap per battery model  $m$  can be made each period.

Constraints (3-13) limit the total batteries in charging by the total number of available chargers  $N$ , while (3-14) establish the batteries minimum ( $\underline{R}_m$ ) and maximum ( $\bar{R}_m$ ) charging power rate in case they are in charging ( $K_{t,m,b} = 1$ ). Equations (3-15) show the composition of the BSS charging power, which may come both from the PV generation ( $P_{t,m,b}^{PV}$ ) or from the grid ( $P_{t,m,b}^G$ ).

The PV generation distribution is defined with (3-16), where a part could be directed for the batteries charging ( $E_{t,m,b}^{PV}$ ) or sold to the grid ( $E_t^{PVs}$ ) following the spot price ( $\pi_t$ ). Since there is no limitation involving its use, there is no PV energy spillage being considered. These equations are given in energy measure (KWh), therefore, Equations (3-17) convert  $E_{t,m,b}^{PV}$  values from energy to power rate unit (KW), creating variables  $P_{t,m,b}^{PV}$  based on the time fraction  $D$ .

Equations (3-18) show the composition of the grid power used by the

BSS, with  $Pb_{t,m,b}$  being the portion below the recommended limit by the grid operator ( $L$ ), where Constraints (3-19) represent this limitation, while  $Pa_{t,m,b}$  is the above limit portion, which will pay a  $\delta^+$ % increased price. The variables scope are shown in (3-20)-(3-24) and, at last, 3-25 define the set of constraints that establish a charging control behavior, which will be further detailed in Section 3.1.3.

As previously discussed, Equation (3-6) contain a bilinear product, which was chosen to be treated using McCormick envelopes [26, 27, 28, 29], since for bilinear products comprising binary variables, it is an exact linear relaxation. Therefore, an auxiliary variable  $Y_{t,m,b}$  is created to substitute the bilinear product  $E_{t-1,m,b} \cdot S_{t,m,b}$  from (3-6), introducing together Constraints (3-26) – (3-29) at the mathematical model, thus recasting the MINLP problem as a MILP one.

$$Y_{t,m,b} \leq \bar{E}_m S_{t,m,b} \quad \forall t \in \mathcal{T}, m \in \mathcal{M}, b \in \mathcal{B}_m \quad (3-26)$$

$$Y_{t,m,b} \leq E_{t-1,m,b} \quad \forall t \in \mathcal{T}, m \in \mathcal{M}, b \in \mathcal{B}_m \quad (3-27)$$

$$Y_{t,m,b} \geq E_{t-1,m,b} - \bar{E}_m (1 - S_{t,m,b}) \quad \forall t \in \mathcal{T}, m \in \mathcal{M}, b \in \mathcal{B}_m \quad (3-28)$$

$$Y_{t,m,b} \geq 0 \quad \forall t \in \mathcal{T}, m \in \mathcal{M}, b \in \mathcal{B}_m \quad (3-29)$$

### 3.1.1

#### Literature Formulation Changes

Besides the battery degradation and charging control extensions developed in this work, the initial formulation presented in [18] was adapted in order to incorporate the assumed BSS business model and several modeling aspects.

Overall, the formulation structure was maintained, where it was included a new set of battery types  $m$ , and several constraints were changed in order to consider this new set. Moreover, it was unconsidered the presence of a revenue per swapping process, therefore the parameter  $C^f$  was excluded from the model, since it used to represent a fixed price for replacing a battery unit. Furthermore, parameters associated with energy losses, conversion and efficiency were also not considered anymore.

Along the model constraints, the energy balance between power provided by the grid and PV was adapted in order to increase the PV flexibility, since in [18], during PV generation hours, the BSS was allowed to charge its batteries using only the PV. Following the same idea, the flexibility of power provided by the grid was also increased with the insertion of Constraints (3-18) – (3-19), allowing the grid limitation  $L$  to be surpassed with a price increase of  $\delta^+$ %.

At last, in reference of the model from [18], Constraints (15) and (19) were also removed, since the first one takes use of a rough approximation for the charging limitation due to SoC increment, while the second use wasn't used in the optimization process, since the SoH wasn't even mathematically defined.

### 3.1.2

#### Battery Degradation Model

Batteries are the main resource of a BSS and there are inherent associated costs to their use that must be considered as operational costs. Besides their acquisition capital, there exists operating costs associated to the battery degradation process, since at long term they bring the necessity of battery replacement. The most severe consequence of batteries degradation is their capacity fading, which happens due to battery calendar and cycle aging. The first one refers to batteries inherent degradation over time, while the second one is the life lost each time the battery cycles between charging and discharging [30].

Overall, the battery degradation rate depends on several factors such as charging and discharging cycles, aging, discharge depth, temperature, and also on its current State of Health (SoH), composing a non linear and complex process. Address a feasible mathematical model that accurately represents the battery degradation cost is a critical challenge in the existing literature, however it is fundamental for more realistic model applications. In this sense, this research takes base on [23] obtained results and develops a linear battery capacity degradation rate model based on charging current profile, which will be detailed further on.

Since energy sellback to grid is not the focus of this study, as it is limited to PV generation, overall the BSS can only control the batteries charging profile, where the discharge process is dependent on EV costumers use, therefore unknown to the BSS. On the other hand, following the same idea, Gao et al. [23] developed a Lithium-ion battery capacity degradation rate model based on the charging profile, which fits well for the present BSS operation model. Based on several experiments, the authors developed a general curve for battery degradation based on the used charging rate and the battery actual capacity loss, i.e, their State of Health (SoH).

Since the original capacity degradation values were based on a complete battery cycle using a constant charging and discharging rate, the obtained degradation values are also based on the same corresponding charging time, which will be commonly different from the adopted time steps at the mathe-



mathematical model. Furthermore, the present study develops a model that considers different time intervals, where in each step the charging rate is decided again and can be changed, thereby raising the necessity of a normalization on the degradation values, making them proportional to the model time step. Therefore, an adaptation on the degradation rate values provided in [23] is proposed over below, fitting them considering the chosen time step discretization upon the day hours and the batteries SoH. Moreover, in the same work, it was provided degradation curves for batteries capacity loss states of 10,20,30 and 40%, however, for this study it is assumed that all BSS batteries have the same capacity loss state and it is equal to 10%.

Further on, taking the 10% capacity loss battery values and the chosen time step of 15 min, Table 3.1 exemplifies the used normalization method. The Charging time column represents the equivalent time for a full charge with the correspond charging rate (C), while the column Factor represents the proportion of the charging time to the time step value. For exemplo, the first line, of 0.5C, represents a full charging time of 120 min, which is 8 times greater than the 15 min time step, which makes the factor being  $\frac{120}{15} = 8$ , therefore the normalized degradation value is  $\frac{0.03419\%}{8} = 0.00427\%$ .

Table 3.1: Battery Degradation Adaptation

Charging Rate (C)	Degradation (10 %)	Charging time (min)	Factor	15min Degradation (10 %)
0.5	0.03419	120	8	0.00427
0.8	0.03756	75	5	0.00751
1	0.04433	60	4	0.01108
1.2	0.05812	50	3.33	0.01744

Given the normalized degradation values, the formed function still follows a non linear curve the same way as the original values. Given the context, it was used a piecewise linear function to approximate the original curve and insert them at the mathematical model. Fig. 3.1 shows the developed linear function based on the same values from Table 3.1. The charging rate values were bound by the same limits of 0.5C and 1.2C as originally used in [23], since the developed curve fit belong to this limit and battery degradation follows a different behavior when near 1.5C. Further details of the battery degradation based on charging rate model can be seen in [23].

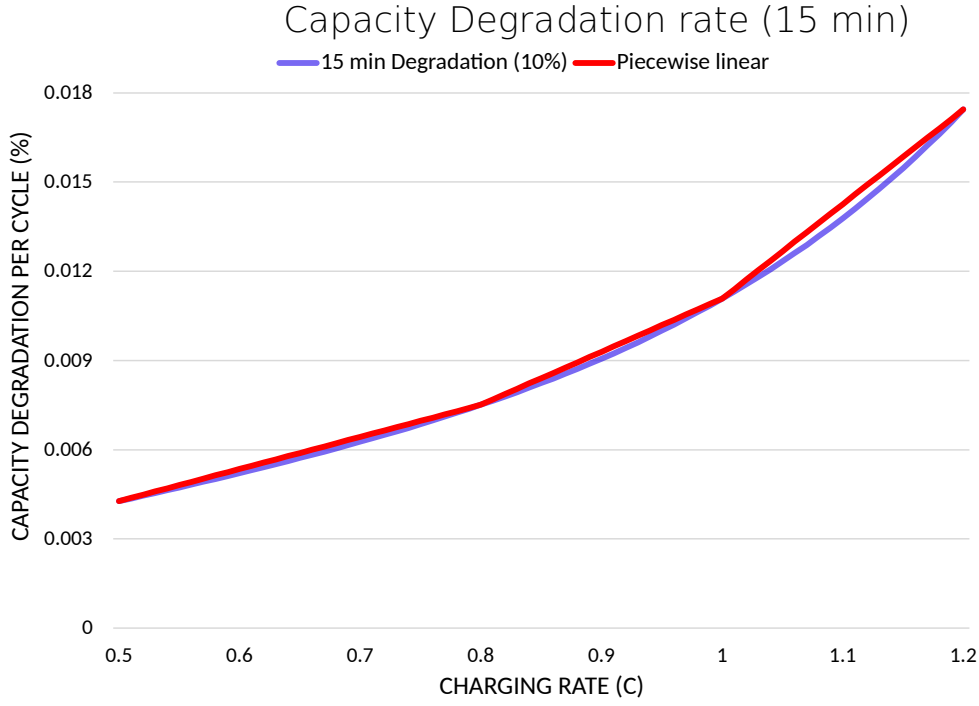


Figure 3.1: Battery degradation curve linearized for 15min time slots

The following set of Constraints (3-31) – (3-36) are used to describe the degradation cost, while Expression (3-30) defines the function  $\phi(K)$ , which is added at the objection function in order to incorporate the battery degradation as an operational cost.

Sets and Indexes (Degradation):

$\Gamma$  Set of linear segments with index  $\gamma$

Parameters (Degradation):

$I_m^{Nom}$ 1C Charging current rate for battery model $m$	$V_m^{DC}$ Volts of direct current for battery model $m$
$\alpha_\gamma$ Angular coefficient of segment $\gamma$	$\beta_\gamma$ Linear coefficient of segment $\gamma$
$C_m$ Battery $m$ acquisition capital cost	$\bar{\theta}$ Maximum % degradation value
$\underline{I}^C$ Minimum established C-Charging rate	$\bar{I}^C$ Maximum established C-Charging rate

Decision Variables (Degradation):

$\theta_{t,m,b}$ % degradation per cycle for battery $b$ , model $m$	$I_{t,m,b}^C$ C-Charging rate for battery $b$ , model $m$
--	---

Objective Function (Degradation):

$$\phi(K) = \sum_{t \in \mathcal{T}} \sum_{m \in \mathcal{M}} \sum_{b \in \mathcal{B}_m} \frac{C_m \theta_{t,m,b}}{2} \quad (3-30)$$

Subject to:

$$P_{t,m,b}^T = V_m^{DC} I_{t,m,b} \quad \forall t \in \mathcal{T}, m \in \mathcal{M}, b \in \mathcal{B}_m \quad (3-31)$$

$$I_{t,m,b} = I_{t,m,b}^{Nom} I_{t,m,b}^C \quad \forall t \in \mathcal{T}, m \in \mathcal{M}, b \in \mathcal{B}_m \quad (3-32)$$

$$\underline{I}^C K_{t,m,b} \leq I_{t,m,b}^C \leq \bar{I}^C K_{t,m,b} \quad \forall t \in \mathcal{T}, m \in \mathcal{M}, b \in \mathcal{B}_m \quad (3-33)$$

$$\theta_{t,m,b} \geq \alpha_\gamma I_{t,m,b}^C + \beta_\gamma K_{t,m,b} \quad \forall t \in \mathcal{T}, m \in \mathcal{M}, b \in \mathcal{B}_m, \gamma \in \Gamma \quad (3-34)$$

$$\theta_{t,m,b} \leq \bar{\theta} K_{t,m,b} \quad \forall t \in \mathcal{T}, m \in \mathcal{M}, b \in \mathcal{B}_m \quad (3-35)$$

$$I_{t,m,b}, I_{t,m,b}^C, \theta_{t,m,b} \geq 0 \quad \forall t \in \mathcal{T}, m \in \mathcal{M}, b \in \mathcal{B}_m \quad (3-36)$$

Expression (3-30) counts the battery degradation cost by  $C_m \theta_{t,m,b}$  value, which is directly related to battery type  $m$  capital cost  $C_m$ , since expensive batteries must have proportionally higher degradation cost. Equations (3-31) relate the charging power with the charging current based on the volts of direct current of the respective battery model ( $V_m^{DC}$ ).

Constraints (3-32) relate the charging current with the respective C-rate ( $I_{t,m,b}^C$ ) based on the nominal current ( $I_{t,m,b}^{Nom}$ ) of 1C, while (3-33) bound the C-rate limits. Constraints (3-34) establish the degradation percentage  $\theta_{t,m,b}$  based on the C-rate value  $I_{t,m,b}^C$  through a piecewise linear function with  $\alpha_\gamma$  and  $\beta_\gamma$  coefficients, while Constraints (3-35) bound the  $\theta_{t,m,b}$  values up to  $\bar{\theta}$ , took as the maximum value of the respective degradation curve, according to the charging status  $K_{t,m,b}$ . Moreover, according to Constraints (3-34) - (3-35), the value of  $\theta_{t,m,b}$  will be nulled in cases where the battery is not being charged. The variables scope are shown in (3-36).

### 3.1.3

#### Charging Control Constraints

The basic formulation aims at deciding the batteries' optimal charging schedule such that the BSS daily profit is maximized. As the day passes, multiples swapping services are realized while stored batteries are being charged for future EV costumers. Furthermore, each serviced costumer leaves a battery with a remaining energy level, therefore increasing the variability of energy level along the BSS storage. In this context, it would be common to see multiple feasible solutions of charging schedule that leads to the same

costumer attendance. However, these multiple solutions can enable unwanted behaviors in the charging schedule, which can include repeatedly turn on and off movement on the chargers. Fig. 3.2 exemplifies the cited situation, which retracts a possible result of the basic model formulation and there is a constantly change in the charger use along the hours.

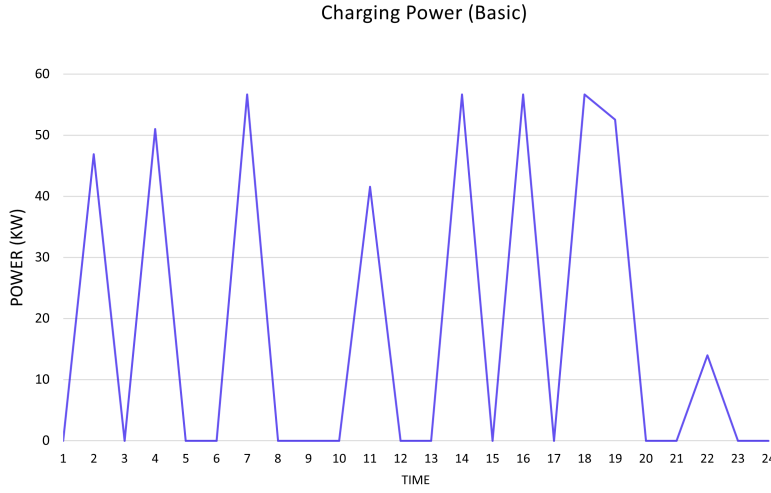


Figure 3.2: Charging Power (Basic)

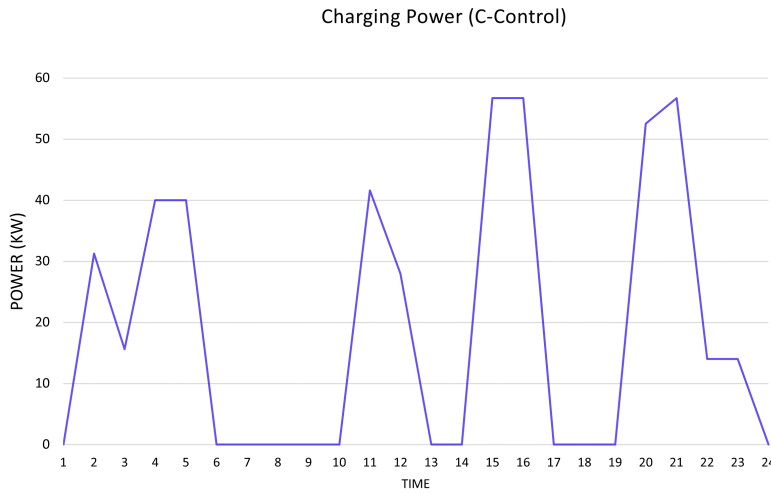


Figure 3.3: Charging Power (C-Control)

A charging schedule containing multiples turn on/off movements can decrease the chargers' lifespan, as well as increase the schedule implementation difficulty. Given the cited problems for the basic formulation, a model extension is proposed by constraints (3-37) – (3-39) insertion together with variables  $U_{t,m,b}$  and  $V_{t,m,b}$ , therefore creating the set  $\Omega$ . The new constraints propose a sequence of logical relationships to disable the charging profile observed in Fig. 3.2, mainly establishing that only one charging process must occur between

two battery swapping for the same battery index  $b$ . The expected behavior can be seen in Fig. 3.3, where the charging profile is smoother and there are less chargers shutdowns. Ahead on the Numerical Experiments section this extension will be further evaluated. The remaining of the section will explain the new proposed variables and constraints.

$U_{t,m,b}$ Charging stopped status for battery $b$ , model $m$	$V_{t,m,b}$ Charging allowance for battery $b$ , model $m$
---	--

$$\Omega = \left\{ (K_{t,m,b}, K_{t-1,m,b}, S_{t-1,m,b}) \in \{0, 1\}^3 \mid \begin{aligned} &\exists (V_{t,m,b}, U_{t,m,b}) \in \{0, 1\}^2; \\ &K_{t,m,b} \leq K_{t-1,m,b} + V_{t,m,b} \quad (3-37) \\ &U_{t,m,b} \geq K_{t-1,m,b} - K_{t,m,b} \quad (3-38) \\ &V_{t,m,b} \geq V_{t-1,m,b} - U_{t,m,b} + S_{t-1,m,b} \end{aligned} \right\}. \quad (3-39)$$

Constraints (3-37) establish that a charging battery can maintain being charging if it was being charged last stage ( $K_{t-1,m,b} = 1$ ) or if it has the allowance ( $V_{t,m,b} = 1$ ) to start charging. On the other hand, Constraints (3-38) establish that when a battery stops being charged ( $K_{t-1,m,b} = 1, K_{t,m,b} = 0$ ), it forces  $U_{t,m,b} = 1$ . Finally, Constraints (3-39) establish that a battery acquires a charging allowance ( $V_{t,m,b} = 1$ ) if it already obtained it before ( $V_{t-1,m,b} = 1$ ) or if it already stopped being charged previously ( $U_{t,m,b} = 1$ ) and a swapping request for it has been accepted ( $S_{t,m,b} = 1$ ). Overall, these constraints establish that only one charging cycle occurs between two accepted swapping requests for the same battery index  $b$ , disabling multiples turn on/off movements during the process while maintaining flexibility in the charging power. Moreover, it is not mandatory that the charging cycle must finish immediately before the swapping process.

## 4

### Case Study

This section presents four case studies developed to investigate the effectiveness of the proposed model and study the optimized decisions, bringing insights about the BSS daily operation in different contexts. Both extensions of battery degradation and charging control are analysed upon their impact at all cases results, as well as sensitivities are realized in order to evaluate the impact of BSS energy precification, number of operating batteries and PV installed capacity.

The case studies mix real and generated data based on historical data from the AECO zone from PJM marketplace [31]. The historical data contemplates real-time price and irradiation rate information based on January and July from 2019 year. Data setup and treatments are further explained in the next sections.

The formulation was implemented using the Julia language 1.6.4 with the support of JuMP<sup>®</sup> 1.1.1 package and Gurobi<sup>®</sup> 9.5.1 Optimizer. All results are obtained on an Intel<sup>®</sup> i7-10700K 3.8GHz processor and 64GB of RAM.

#### 4.1

##### Data Setup

The proposed case studies take use of BSS configuration data, which will be equal in all cases and includes BSS infrastructure information such as number of chargers. This information is presented in Table 4.1. The  $L$  value is took as approximately 35% of the power provided by all chargers at maximum power rate. Moreover, due to operation rules, it was also considered that all BSS batteries start and finish the day completely full.

Table 4.1: BSS General Configuration

Parameters	Value
$D$	1/4
$SOC^{t_f}$	100%
$N$	5
$L$	170 kW
$\delta^+$	5%

The remaining parameters were extracted from real databases or generated following consistent values or probability distributions. The remaining of the section will present all data setup involved at the case studies development.

#### 4.1.1

##### Traffic and Arrivals Data

The EVs time arrival data were considered to be previously known at beginning of the day and were generated based on the USA urban traffic data divided into weekdays and weekends, available at [32] and represented by Fig. 4.1. Although the data belongs to 2011, the urban traffic profile shall remain the same, where the peak hours occur during work time and decreases by night. Since the EV arrivals are described by binary values for each battery model type with the  $A_{t,m}$  matrix, the Bernoulli distribution with an hourly variable probability was used for the values generation. The maximum traffic hours were associated with a maximum arrival probability, as well as the minimum ones were associated to a minimum arrival probability. The middle hours probability values were calculated with a linear interpolation. The maximum and minimum EV arrival probabilities assumed were 70% and 5%, respectively.

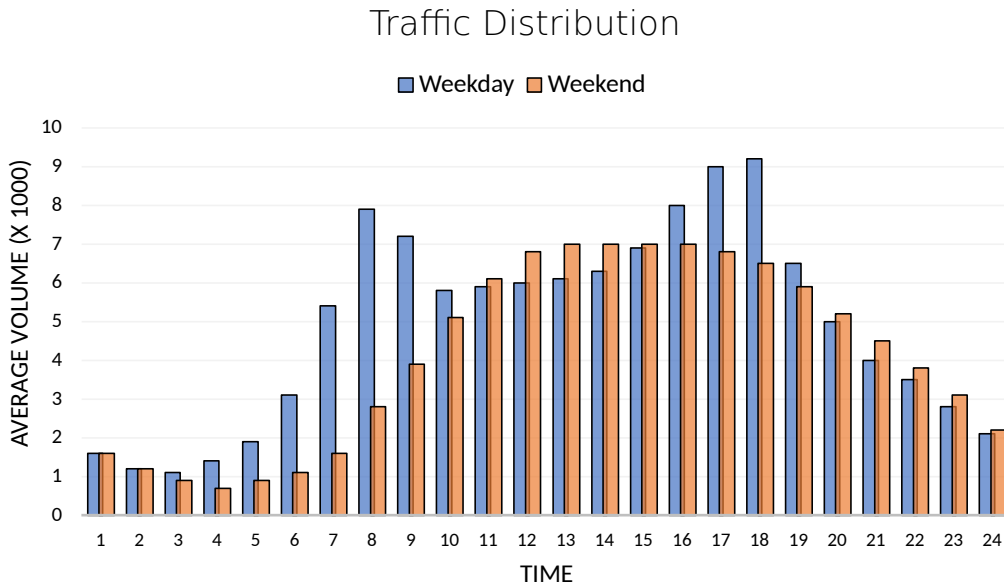


Figure 4.1: USA Hourly Urban Interstates Traffic Distribution

The EV costumers data related to the battery remaining energy level by arrival time ( $E_{t,m}^{EV}$ ), as well as their minimum desired energy level to accept the swapping of the depleted battery ( $\tilde{E}_{t,m}$ ) are also considered to be known and were generated with random values. The first one followed values between 5%

and 30 % for respective battery SOC, while the second one remained between 70% and 100 %.

#### 4.1.2

##### PV Generation

The PV generation power values were generated using the Time Series Lab (TSL), a renewable modeling tool developed by PSR company [33] which contains a module that enables the extraction of an irradiation and wind speed historical data based on a 40 years global reanalyses database provided by MERRA-2 or ERA-5 sources, where the first one is used in this work. Based on the renewable source geographic location, his type, attributes and additional information, varying from solar to wind plants, the TSL executes the appropriate conversion to transform irradiation and wind speed data into generation values. The TSL also contains a module that generates synthetic scenarios based on the converted generation historical data, however it is not used in this work. It was assumed a PV panel with a installed capacity of 500 KW, zero tracking axis and a AC/DC ratio conversion of 1.1.

Fig. 4.2 displays the PV profile along the January and July, where the impact of weather stations in PV expected generation can be clearly seen. Furthermore, the production factor difference of both months quantifies the differences, where January owns a 0.06 average production factor, while July has 0.23. Although there are hourly PV generation available, the proposed model uses minor time steps, therefore requiring an equivalence of hourly generation for hour fractions generation.



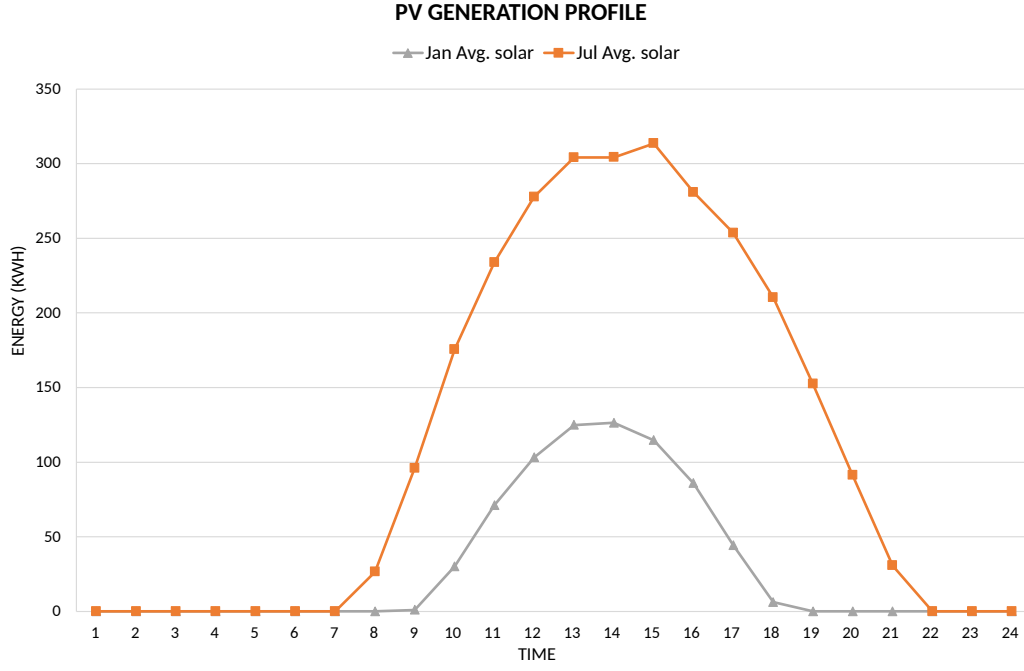


Figure 4.2: PV Power Distribution

In order to put the obtained hourly values into time slots of 15 minutes and consider variability, the PV generation values were decomposed as following: Considering the hour  $h$  with estimated PV generation  $PV^h$ , each decomposed value for the belonging time slot  $t$   $PV_t^m$  and  $\epsilon$  being a random value between -10% and 10%, equation (4-1) shows the proposed hour-minute equivalence.

$$PV_t^m = \begin{cases} \frac{PV^h(1 + \epsilon)}{4} & t = 1 \dots 3 \\ PV^h - \sum_{t'=1}^3 PV_{t'}^m & t = 4 \end{cases} \quad (4-1)$$

The method brings variability within PV generation inside minutes horizon while still keeping the original hour generation, as one possible realization can be seen in Fig. 4.3 with the Jul/2019 PV data.

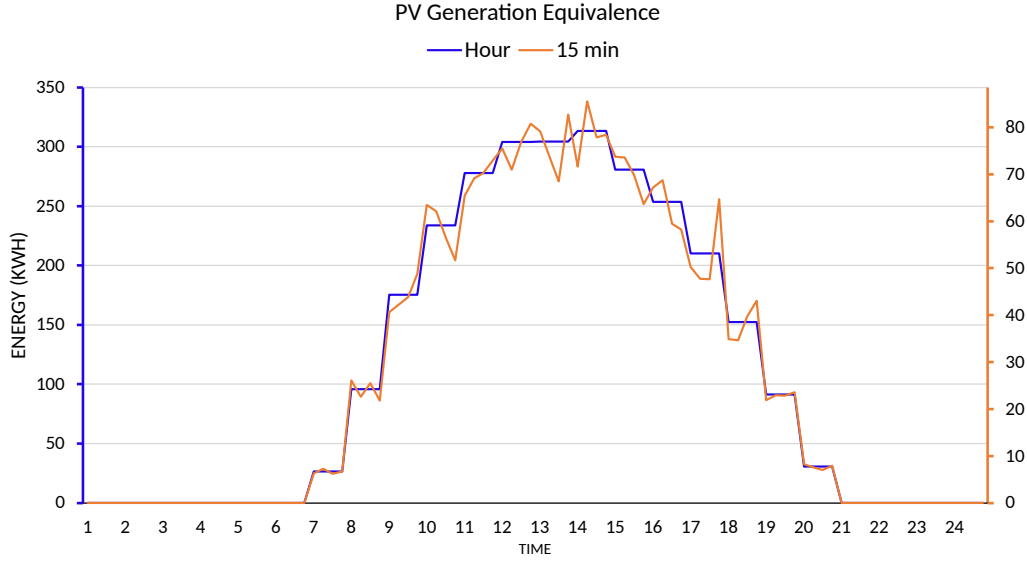


Figure 4.3: PV Generation Distribution in 15 min horizon

### 4.1.3

#### Batteries data

The BSS batteries configuration are presented in Table 4.2. The station operates with a total of 8 batteries and two different types with the same amount. Battery Model 1 represents a Tesla Model Y battery [34], while Model 2 represents a Nissan Leaf Standard [35]. Both battery data are available at the respective manufactures' manual. The power rate values were calculated based on the batteries capacity and the charging rate bounds cited at Section 3.1.2 in order to maintain consistency. Both batteries cost ( $C_m$ ) were estimated based on the Li-Ion battery cost per kWh of 2019 provided by Reka et al. study [36], thereby adopting a cost of \$200 per KWh. Finally, the nominal voltage of direct current values ( $V_m^{DC}$ ) were also took from manufacturer's.

The remaining battery data relative to the proposed degradation model ( $I_{Min}^C, I_{Max}^C, \theta^{Max}$ ) is already cited in Section 3.1.2.

Table 4.2: BSS Batteries Configuration

Parameters	Value ( $m = 1$ )	Value ( $m = 2$ )
$B(m)$	4	4
$\bar{E}_m$	67 KWh	40 KWh
$\bar{R}_m$	80.4 KW	48 KW
$\underline{R}_m$	33.5 KW	20 KW
$C_m$	\$13400	\$8000
$V_m^{DC}$	360	360
$I_m^{Nom}$	0.186 A	0.111 A

#### 4.1.4

##### Energy price

The energy market price information were took from the PJM database [31] based on the real-time hourly price from AECO zone. The average hourly price was calculated for the weekdays and weekends of the selected horizon, thereby bringing different price profiles for the study. Fig 4.4 shows the energy price curves, reflecting their differences according to the day type and associated month. During the cases model execution, the prices were brought into the 15 minutes time slots only repeating the respective hour price.

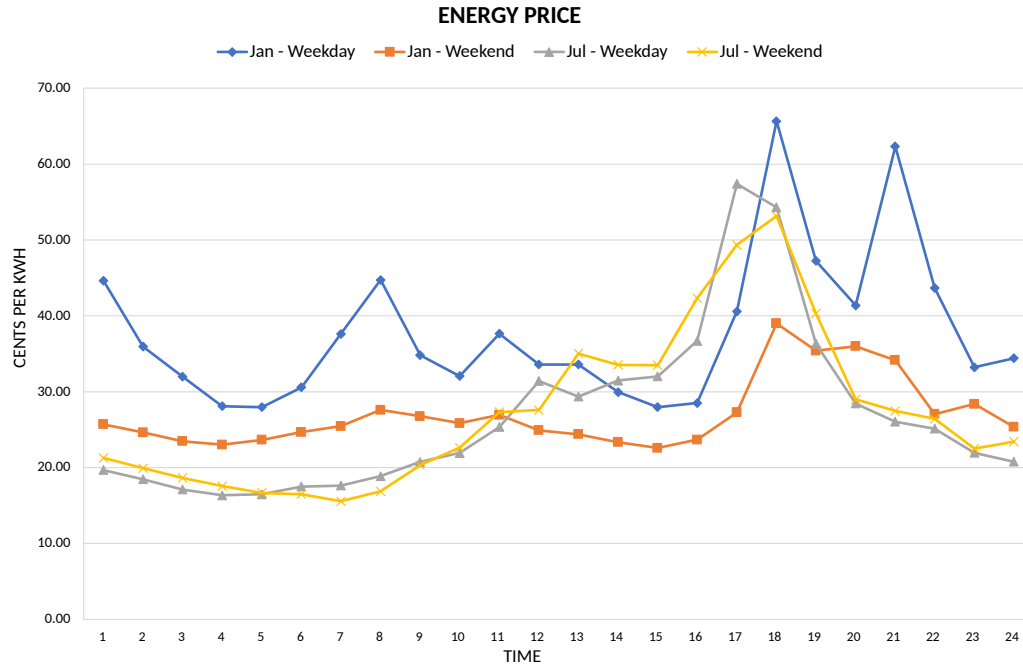


Figure 4.4: Average Hourly Real Time Energy Price by AECO zone in 2019

## 4.2 Cases Description

Given the presented data setup and all involved assumptions, 4 case study types are developed in order to evaluate the proposed model at different situations based on the historical data of PJM AECO zone. For each case study type it was generated 3 instances, summing up to 12 cases to be evaluated by the proposed methodology. Table 4.3 showcase the cases description summary, where each one involves different interaction between the available information, i.e, the traffic data, PV generation and energy price profile. The cases are generated based on typical weekdays and weekends, since the traffic and energy time profile follow different pattern, while the January and July months represent the winter and summer weather, respectively, providing variability on both expected PV generation and also energy price profile.

Each case instance is described in Table 4.4 together with their assumed EV arrivals, which were generated based on the traffic curves described in Section 4.1.1, making use of the described probabilities along the traffic profile for the respective typical day, where each arrival is considered as an independent random variable. Overall, in average, the developed cases presented an expected total EV arrivals of 60, therefore the aspect that differs then is the distribution of these arrivals along the day, which follows the respective traffic curve profile.

Table 4.3: Study Cases Description Summary

Case	Typical Day	Month	$\lambda$ (\$)
1	weekday	Jul	26.04
2	weekend	Jul	27.47
3	weekday	Jan	37.62
4	weekend	Jan	26.76

Table 4.4: Cases Instances Arrivals Summary

Case	Instance	Arrivals ( $m = 1$ )	Arrivals ( $m = 2$ )	Total
1	A	33	29	62
1	B	28	31	59
1	C	29	28	57
2	A	32	29	61
2	B	35	33	68
2	C	32	29	61
3	A	28	30	58
3	B	27	25	52
3	C	33	27	60
4	A	31	33	64
4	B	30	34	64
4	C	26	32	58

Accordingly to the respective month, the price per swapped battery  $\lambda$  is formed as the 60th percentile of the energy price hours along the day, thereby encouraging the BSS to sell batteries with a reduced value regarding the peak price.

### 4.3 BSS Metrics

In order to measure the performance of the BSS operations, five metrics were developed focusing on aspects such as costumers attendance and equip-

ment use, thereby enabling useful information gathering for BSS operators. We would like to highlight that, these metrics can also be used to create high-level insights on the BSS sizing and expansion plan. Further below the metrics are described along with their respective mathematical formulation in (4-2) – (4-6).

<b>Service Level (SL<sub>m</sub>):</b> Percentage of serviced swapping requests (4-2)
<b>Charger Use (ChU<sub>t</sub>):</b> Percentage use of the BSS chargers (4-3)
<b>Charger Power Use (ChPU<sub>t</sub>):</b> Percentage use of the BSS chargers maximum power rate (4-4)
<b>Power Above Use (PA<sub>t</sub>):</b> Percentage of used grid power above the recommended limit (4-5)
<b>PV Sold Energy (PVS):</b> Percentage of PV sold energy (4-6)

$$SL_m = \frac{\sum_{t \in \mathcal{T}} \sum_{b \in \mathcal{B}_m} S_{t,m,b}}{\sum_{t \in \mathcal{T}} \sum_{b \in \mathcal{B}_m} A_{t,m}} \quad \forall m \in \mathcal{M} \quad (4-2)$$

$$ChU_t = \frac{\sum_{m \in \mathcal{M}} \sum_{b \in \mathcal{B}_m} K_{t,m,b}}{N} \quad \forall t \in \mathcal{T} \quad (4-3)$$

$$ChPU_t = \frac{\sum_{m \in \mathcal{M}} \sum_{b \in \mathcal{B}_m} P_{t,m,b}^G}{\bar{R}_m} \quad \forall t \in \mathcal{T} \mid K_{t,m,b} = 1 \quad (4-4)$$

$$PA_t = \frac{\sum_{m \in \mathcal{M}} \sum_{b \in \mathcal{B}_m} Pa_{t,m,b}}{\sum_{m \in \mathcal{M}} \sum_{b \in \mathcal{B}_m} P_{t,m,b}^G} \quad \forall t \in \mathcal{T} \quad (4-5)$$

$$PVS = \frac{\sum_{t \in \mathcal{T}} E_t^{PVS}}{\sum_{t \in \mathcal{T}} E_t^{PV}} \quad (4-6)$$

Along with the described metrics, it is important to consider the customer attendance along with the delivered energy level by the batteries. According to the problem assumptions, costumers are willing to receive batteries fully charged, yet they accept partially charged ones considering that the BSS may have difficulties to deliver complete batteries to all costumers. Therefore, considering two BSS situations with the same service level, the one that delivered fully charged batteries more frequently or above the minimum acceptable energy level for each customer will be classified as better. Considering this business model aspect, the following metric is proposed in order to increase the operation performance detailing:

**Full Batteries (FB):** Percentage of serviced swapping requests with full batteries

It should be highlighted that  $ChPU_t$  metric only considers charging batteries, thereby not including stages of batteries in swapping status, which would include null values at the metric average value. Apart from the metrics proposed in this section, the cases are also evaluated based on the net revenue distribution, which is composed by the sold PV energy and the revenue relative to the realized swapping process along the day.

## 5

### Numerical Experiments

This section provides a descriptive analytics of the numerical experiments performed with the proposed model with the setup, cases and BSS metrics described in Section 4. Furthermore, the proposed model extensions are individually evaluated in each case setup and all numerical experiments were optimized with a time limit of 1 hour. We highlight that, as previously said in Section 3, it will be assumed that all requests will be accepted, thereby establishing a Service Level of 100%.

#### 5.1

##### Case Studies Overview

Making use of the complete model version, which includes both degradation and charging control extensions, all developed cases were optimized and their results are presented in Table 5.1. Values from columns 3 – 6 are given in dollar unit, while from column 7 to 12, all values are given in percentages. In order to present an overview of each case type, Table 5.2 summarizes the results taking the average value of all instances for each case.

Results indicate that, overall, the BSS profit is composed by the swapping profit, i.e., the profit involved at the EVs battery swapping service, which is represented by the third column, together with the PV profit, which is shown at the fourth column. The degradation cost is indicated in the fifth column and is treated as a referential cost, since it is related to the future necessity of battery replacement, so not being an immediate cost as the charging cost, which is incorporated in the swapping profit. Although the degradation is not considered as an immediate cost, its consideration in the mathematical model as an operational cost influences the profit maximization. More details in these aspects will be given in Section 5.2. The remaining columns present the value of the metrics for the given solution, excepts for Column 7 where the solution GAP is shown.

Fig. 5.1 summarizes the case studies results over the operational profit aspect, which are divided in swapping and PV profit. The degradation is considered as a reference operational cost, since its consideration in the problem extends the battery lifetime with an optimized charging profile, however, due not being an immediate cost, it is not counted to the BSS daily profit. Moreover, for each case study, the obtained total operational profit is highlighted at the top of the charts, where Case 1, the most profitable one,



Table 5.1: Case studies results

Case	Instance	Profit	Swp. Profit	PV Profit	Degrad.	GAP	ChU	ChPU	PA	PVS	FB
1	A	802.76	242.42	560.34	82.47	0.89	68.44	27.76	1.45	61.31	22.26
1	B	834.87	242.39	592.48	80.71	1.35	67.19	30.02	0.06	62.58	27.62
1	C	833.29	173.41	659.88	75.50	1.47	62.81	35.87	1.88	72.48	26.79
2	A	830.59	366.98	463.61	82.74	1.36	65.00	24.38	0.00	50.28	23.01
2	B	787.05	337.25	449.80	93.63	1.34	68.13	27.92	1.19	50.97	19.26
2	C	839.61	320.54	519.07	84.35	1.31	64.06	26.01	0.14	56.50	24.73
3	A	283.38	187.98	95.40	84.59	4.06	64.38	41.38	6.07	38.47	34.04
3	B	255.51	151.28	104.23	75.90	3.15	56.88	41.45	5.00	42.30	40.06
3	C	255.81	161.66	94.15	84.79	3.91	65.00	41.86	8.08	39.18	38.23
4	A	170.27	97.16	73.11	83.11	4.11	68.44	39.08	8.96	40.87	12.51
4	B	172.09	115.78	56.31	84.76	4.59	66.88	40.18	9.31	31.19	14.22
4	C	188.82	121.65	67.17	71.26	3.75	62.19	39.89	6.96	37.54	14.14

Table 5.2: Case studies average results

Case	Profit	Swp. Profit	PV Profit	Degrad.	GAP	ChU	ChPU	PA	PVS	FB
1	823.64	219.41	604.23	79.56	1.24	66.15	31.22	1.13	65.46	36.53
2	819.08	341.59	477.49	86.91	1.34	65.73	26.10	0.44	52.58	29.02
3	264.90	166.97	97.93	81.76	3.71	62.08	41.56	6.38	39.98	47.86
4	177.06	111.53	65.53	79.71	4.15	65.83	39.72	8.41	36.54	24.28

is evaluated at \$823.64. Along Cases 1 and 2, where a summer weather is retracted, the BSS profit is mainly composed by PV sale to grid, while Cases 3 and 4 own a predominant profit arising from the swapping service. The battery degradation associated costs are very similar in all cases, except for Case 2, where there is a slightly higher value, indicating a more degradable operation for the batteries.

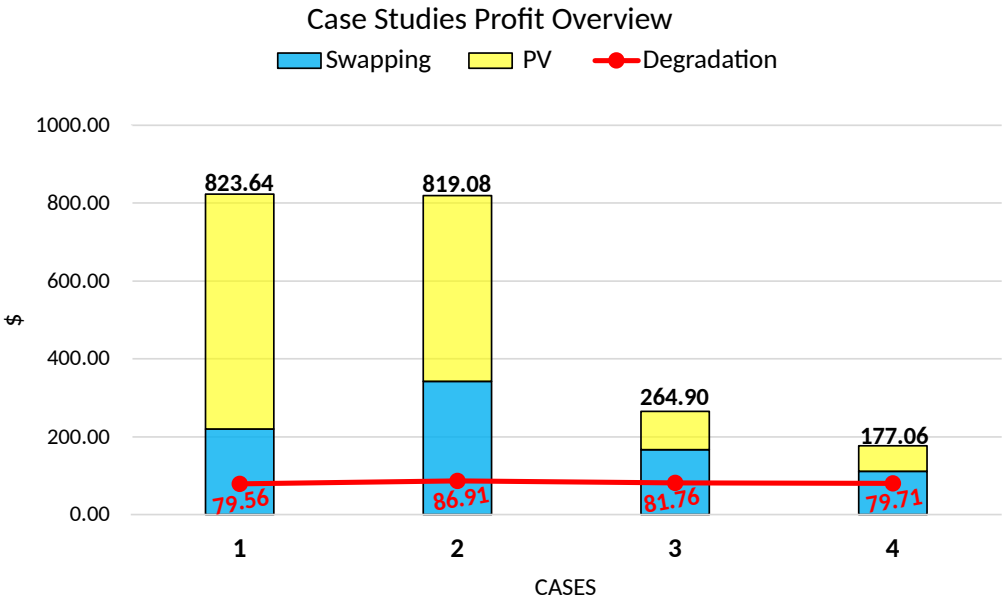


Figure 5.1: Case Studies Profit Overview

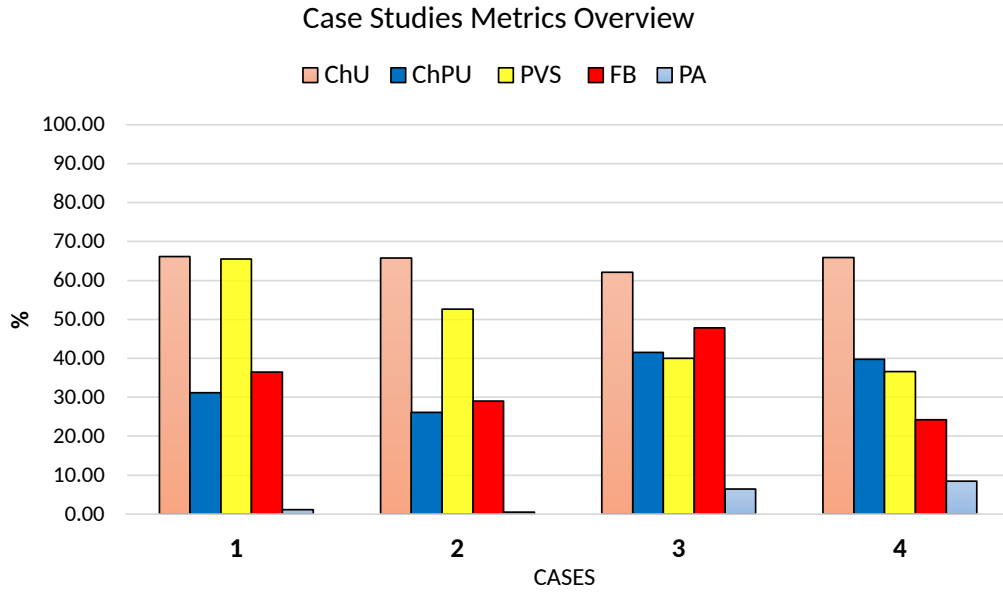


Figure 5.2: Case Studies Metrics Overview

Fig. 5.2, on the other hand, illustrate the case studies metrics overview, which complements the previous analyses on the profit. In proportion with their high PV profit, Cases 1 and 2 also have a high PV sale percentage, which indicates that July's typical energy price curve favours the PV sale at spot prices. According to PA metric, these same cases also presented the lowest values of power above limit, indicating the least-need of more than 170kW power for their optimized operations, which would be helpful for an energy contract planning. Since all cases achieved the same Service Level of 100%, the FB metric is primordial to distinguish the better operations, where is possible to notice Case 3 presenting almost 50% of fully batteries delivery, indicating that winter typical weekday price curve favours the profitability of the BSS energy delivery.

Overall, the results show that high PV expected generation increases the BSS profit, (Cases 1 and 2). Besides the PV generation level due to weather station, Cases 1 and 2 also indicate a energy price profile that mostly favours the PV sale to grid, which is enhanced with the energy storage capability. Cases 3 and 4, on the other hand, show a lower profit, mostly associated to the lower PV generation of the winter, however Case 3 presented the better EV swapping requests attendance in terms of full batteries delivery. It is important to highlight that PV sale profitability is directly associated with the spot price, which also depends on the weather station, especially in energy systems with a great penetration of renewable generation.

## 5.2

### Model Extensions Evaluation

This section provides a comparison between the proposed model extensions and its impact on the empirical/numerical results. All developed case studies are used to evaluate each extension and support a general insights upon the use of both proposed model extensions. For the sake of model notations, the complete model with all extensions is named as final model, while the one without extensions, the simplest one, is named as basic model. Further on, following a similar structure as the previous section, the results will be compared based on both profit and metrics values for each case study. Figs. 5.3 – Fig. 5.10 summarize the obtained results for each case study and each possible combination of the model extensions. Similar as in Section 5.1, each case values are taken as the average value of all solved instances.

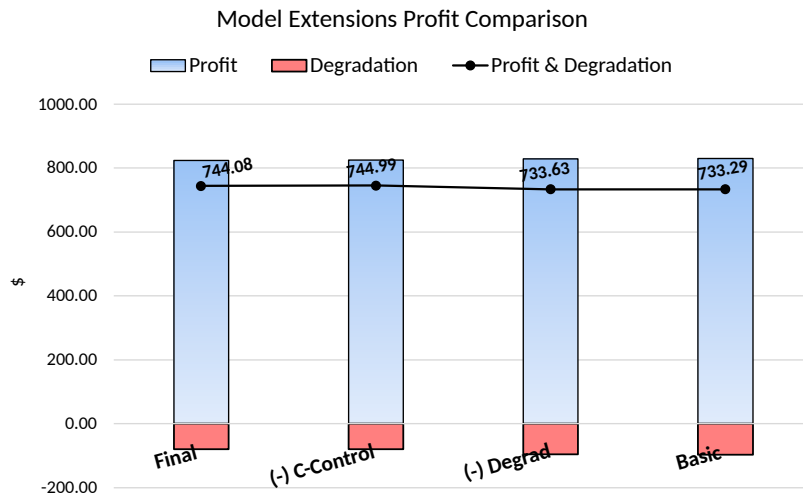


Figure 5.3: Profit Comparison for Case 1

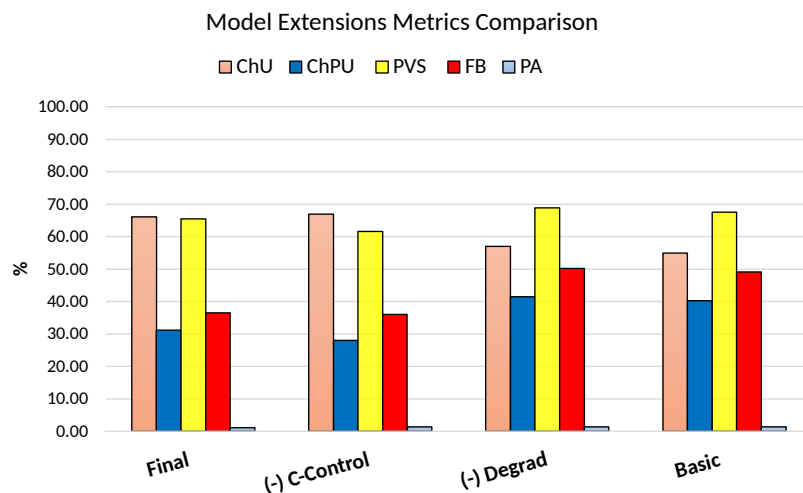


Figure 5.4: Metrics Comparison for Case 1

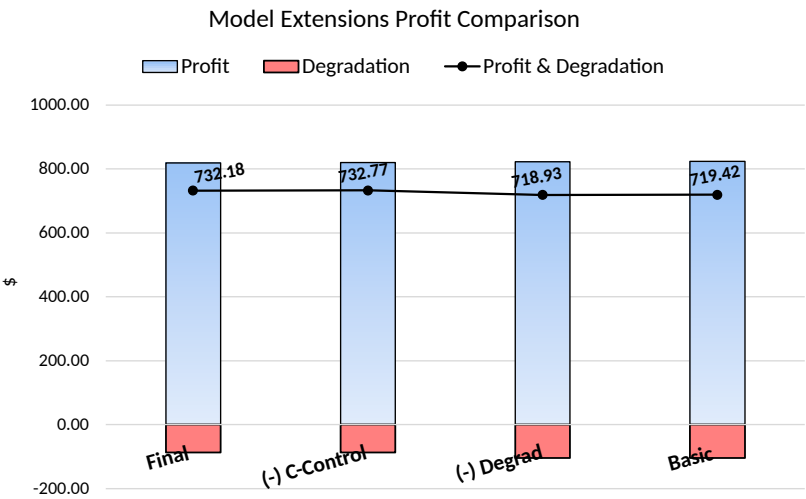


Figure 5.5: Profit Comparison for Case 2

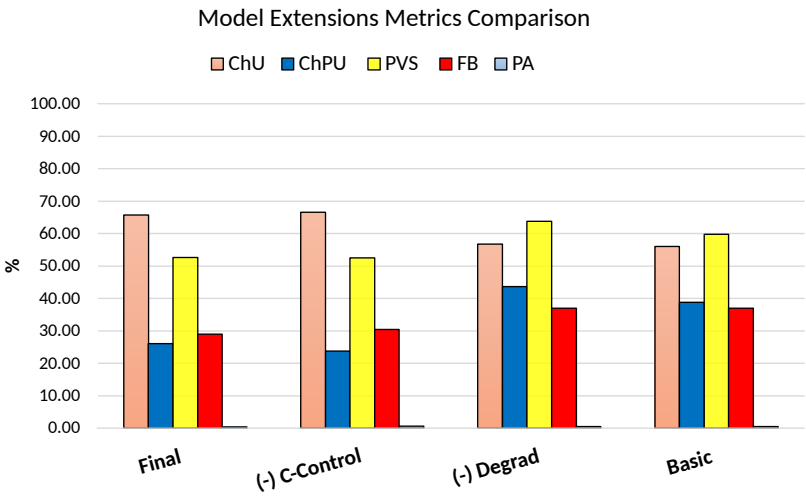


Figure 5.6: Metrics Comparison for Case 2

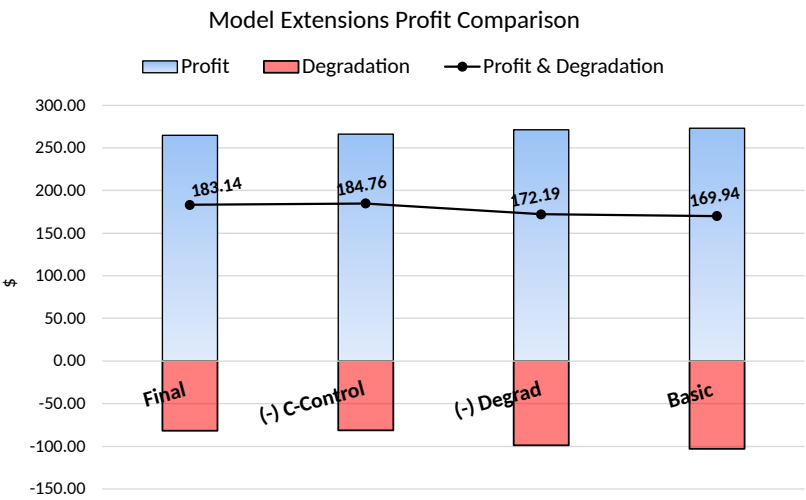


Figure 5.7: Profit Comparison for Case 3

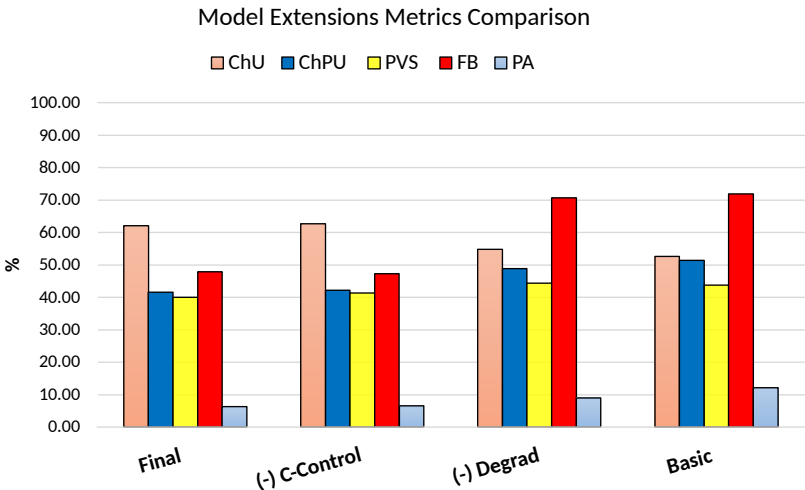


Figure 5.8: Metrics Comparison for Case 3

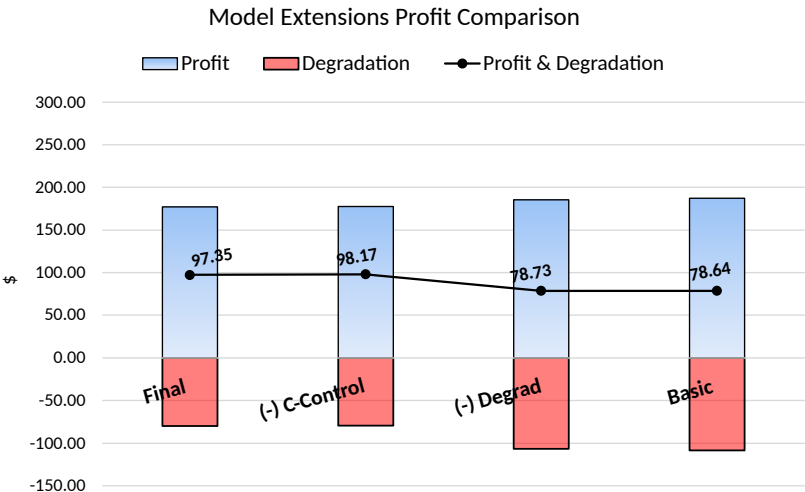


Figure 5.9: Profit Comparison for Case 4

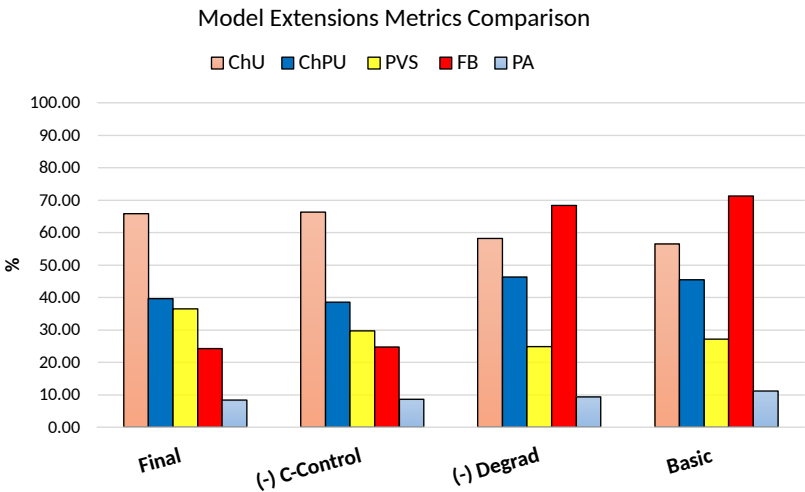


Figure 5.10: Metrics Comparison for Case 4

In all figures the rightmost column shows a result related to the complete model, while each following column to the left updates the result with a removed extension until achieve the most basic model, i.e., disregarding the degradation cost and charging control constraints.

Overall, the obtained results show a behavior on each model extension impact in the profit and metrics results. Under the profit aspect, no considerable changes can be observed among the different combinations, however, when the degradation is considered as an immediate cost (illustrated by the Profit & Degradation curve), the results point to a more profitable operation with the use of the degradation extension. The charging control constraints, on the other hand, slightly change the BSS total profit, while maintaining a smart use of the battery chargers. Although this constraint use points to an extension of the BSS chargers lifetime and an easier real implementation of the solution, the developed metrics are not capable of directly show its benefits, as shown in Figs. 5.4, 5.6, 5.8 and 5.10.

Therefore, by analysing the metrics impact over the model extensions, it is possible to notice the expressive impact of the degradation extension, since it significantly changes the Chargers Power Use and Power Above metric values, especially in Cases 3 and 4, while the PV sale and Chargers use increase. Overall, the results confirm that a BSS operation without considering battery degradation improves the swapping service, since more fully batteries are delivered, however the degradation costs increasing may not compensate this better service. Furthermore, comparing the complete and basic models, Cases 2 and 4 were the least and most affected cases in terms of degradation cost, presenting a reduction of 16% and 26%, respectively. Towards the metrics, the use of the charging control constraints give slightly changes in the charger related metrics, since they change the flexibility of the charging schedule decisions. In this sense, together with the minimal impact in the profit values, it is possible to conclude that the use of these constraints bring more benefits to the BSS solution.

Both proposed model extensions evaluated at this section point towards a benefit for the BSS operations, especially at battery lifetime management, reducing the need for battery replacement in the long term, as well as chargers lifetime management and simpler schedule real implementation with the charging control extension.

### 5.3

#### Case 1 Analyses

Case 1A is selected to be further detailed at this section due to its representativeness and higher opportunities to evaluate the developed metrics and other analyses. Being a typical summer weekday amplifies the consideration of its analysis, as well as the higher PV generation enables a higher interaction between the model decision variables. In order to obtain an overview of the station decisions, it will be presented and discussed the optimized decisions of charging schedule, PV energy use, charging power profile, profit distribution, EV requests attendance, all of them evaluated during the horizon of 7AM – 11PM, there the BSS operates. At last, it will be provided an economical evaluation of the BSS towards the costumers perspective.

#### 5.3.1

##### Charging Schedule

Considering the presented parameters from Section 4.1, the mathematical model has optimized the charge schedule of the batteries, deciding for each period the energy level, battery assignment and the respective charging power. A sample of a charging scheduling over the time can be seen in Fig. 5.11 for Battery 2 of Model 1, while Fig. 5.12 shows for Battery 3 of Model 2. The battery SOC and C-Charging Rate are used in order to unify the analysis with no need to further discuss batteries capacity or maximum charging power rate values.

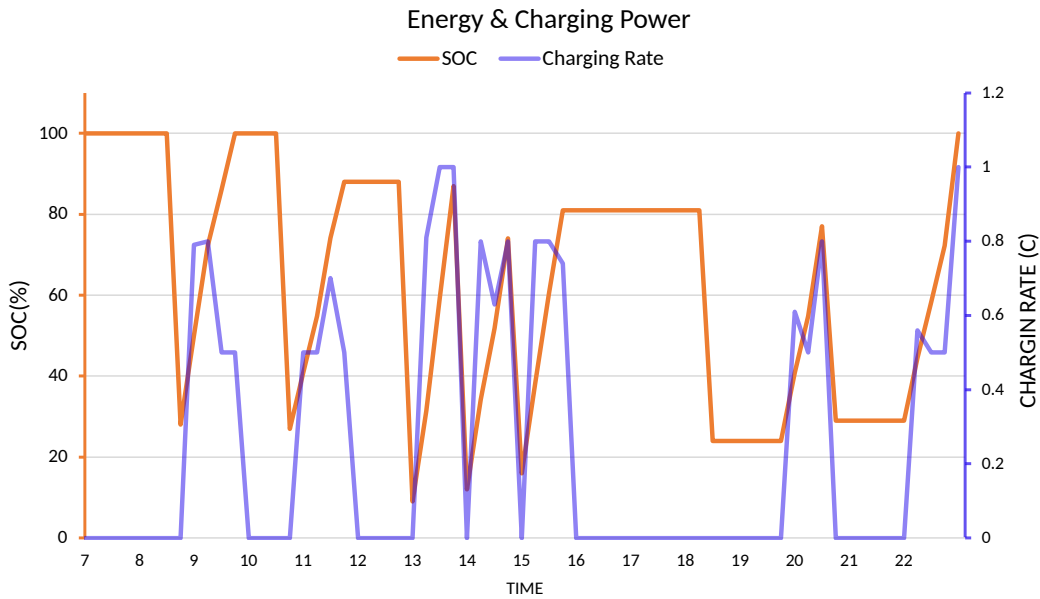
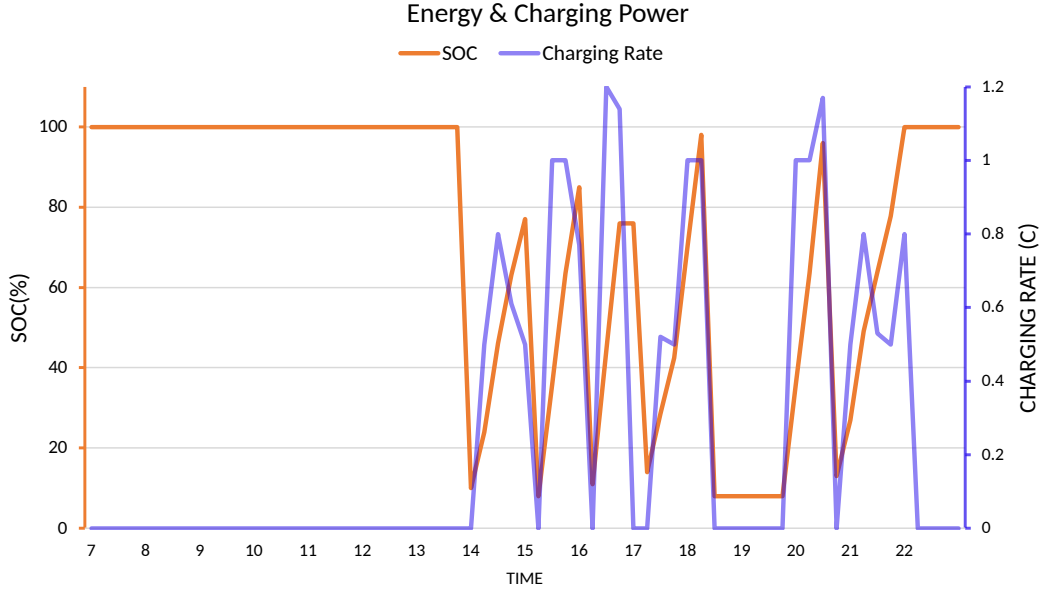


Figure 5.11: Charging schedule for  $m = 1, b = 2$

Figure 5.12: Charging schedule for  $m = 2, b = 3$ 

Each sudden drop of the SOC values indicates the swapping service, where the charged battery is swapped with a depleted one. A visual analysis on both charts show that Model 1 battery has been swapped seven times, being two of them with a full charged battery delivery, while Model 2 battery realized six swaps, with only one fully battery swapping. Moreover, Model 1 battery has been swapped by the day's first hours, with a more sparse swapping frequency along the day, while Model 2 battery has been swapped for the first time around Hour 14 and has a more concentrated swapping frequency between Hours 14 and 19. Both batteries finishes the day at 100% SOC in accordance with the final SOC constraint.

On the other hand, the charging profile also shows considerable differences between the models, where the maximum charging rate achieved for Model 1 and Model 2 batteries were 1C and 1.2C, respectively. Since the proposed degradation cost model is based on the battery capital cost and there is a high curve inflation between 1C and 1.2C charging rate, a cautious charging rate is expected to be seen in these values. However, a charging above 1C may be required in cases of sequentially EV requests for the same model. Overall, Model 1 battery presented a less degrading charging profile in comparison to Model 2 battery, since the average value of their non null charging rate values were 0.69C and 0.8C, respectively.

Finally, the effect of the proposed charging control constraints can be clearly seen, since each battery followed a single charging cycle between two swapping services, thereby increasing the BSS chargers lifespan, even-though



they are not directly evaluated at the mathematical model.

### 5.3.2 PV Energy Use

The selected case study contemplates a typical weekday of the USA summer, where the irradiation rate and PV generation shall be elevated. Along the sunny hours, the BSS can decide to use the PV energy for batteries charging or to grid sale at the spot price. Fig. 5.13 shows the hourly distribution of the PV generation together with the energy price and BSS swapping price per KWh being equal to the 60th percentile of the day energy price. It is possible to notice the mismatch of the peak hour for both curves, thereby providing a mixed solution between PV energy intended to batteries charging and sale to grid.

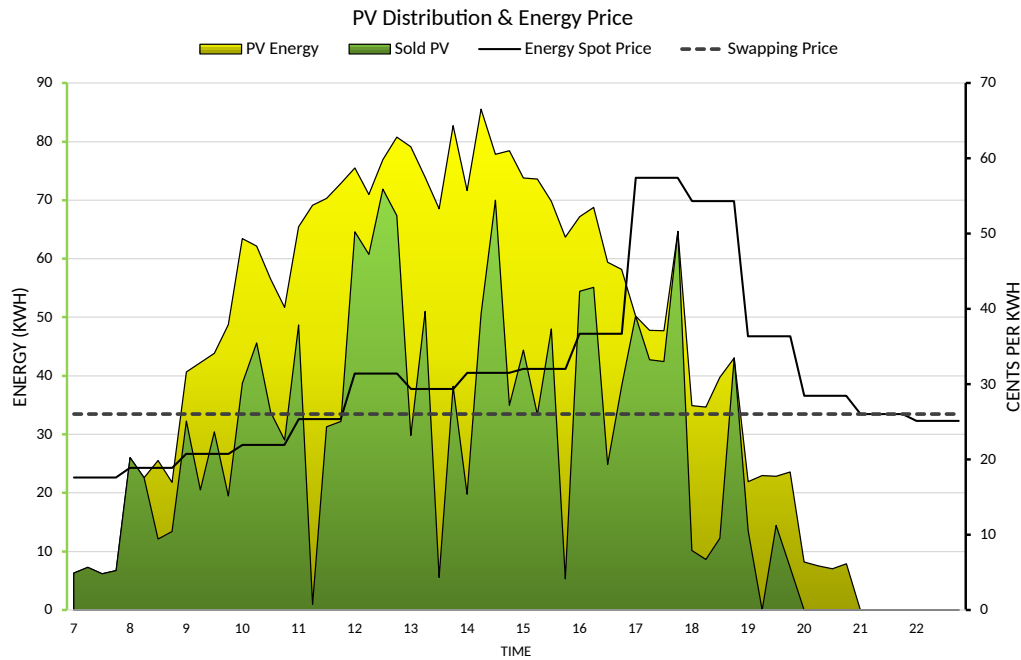


Figure 5.13: PV Energy use and Energy Price

Overall, the maximum profit can be achieved by PV energy sale during the hours where the spot price is above the swapping price, while the remaining hours would be intended for batteries charging. However, besides the most profitable decision, PV energy sale is an easier and more flexible decision, since batteries charging requires the availability of a battery, which depends on the swapping realization in order to obtain depleted batteries in the first hours of the day. Moreover, the use of PV energy can also be associated with the minimization of charging costs, i.e, avoid the use of charging power above

the recommended limit by the grid operator. More details towards this aspect will be given next.

### 5.3.3 Charging Power Profile

Besides having the use of PV energy to support the operation, the BSS often needs to buy energy from the grid in order to attend EV swapping requests, especially in off-peak hours, where the spot-price is at relatively low levels. Fig. 5.14 illustrates the BSS charging profile along the day, where it is possible to see the PV energy function to avoid or reduce the use of grid power in peak hours. We highlight that, instead of imposing a power limit for the grid power provided to the BSS, the present analysis assumes a limit of 170kW that, when surpass, brings a 5% increased price for the charging

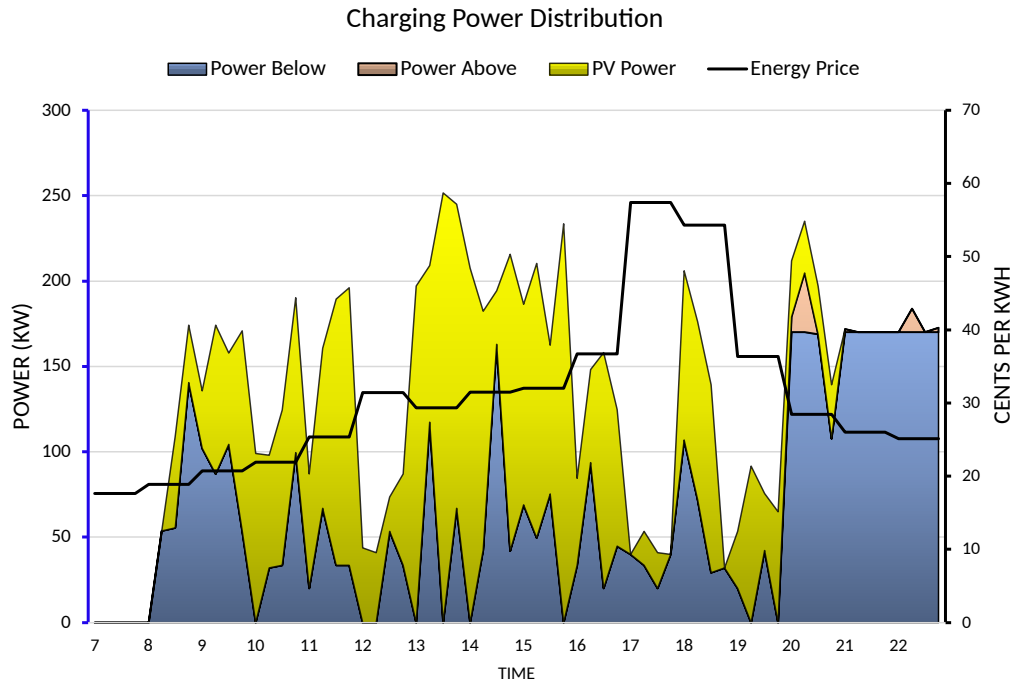


Figure 5.14: PV Use and Energy Price

A few moments of increased cost in power use can be observed by the at the last operating hours – from Hour 20 onward – which can be related to the final SOC constraints together with cheaper energy price. The first hour, on the other hand, does not require grid power since the batteries start the day fully charged, while several hours have a low or even zero power provided by the grid due to PV power presence. The greatest benefit from PV energy can be observed near Hour 14, when there is the peak of PV generation, and Hour 18, when still has PV availability during the peak of energy price.

### 5.3.4 Profit Distribution

Fig 5.15 illustrates the BSS profit distribution, where it is possible to observe the revenue and costs balance. It is noticeable the revenue peak right before Hour 18, where there is a mix between PV generation, and its consequently sale to grid, which is consistent with Fig. 5.13, together with attended swapping requests. Hour 21 onward concentrates the BSS costs associated with batteries charging, exploring the lower energy price in order to finish the day with all batteries at 100%, in accordance with Fig. 5.14 behavior. The degradation cost was not illustrated due to its charging reference use, despite it impacts in the charging profile and reduces the future necessity of battery replacing.

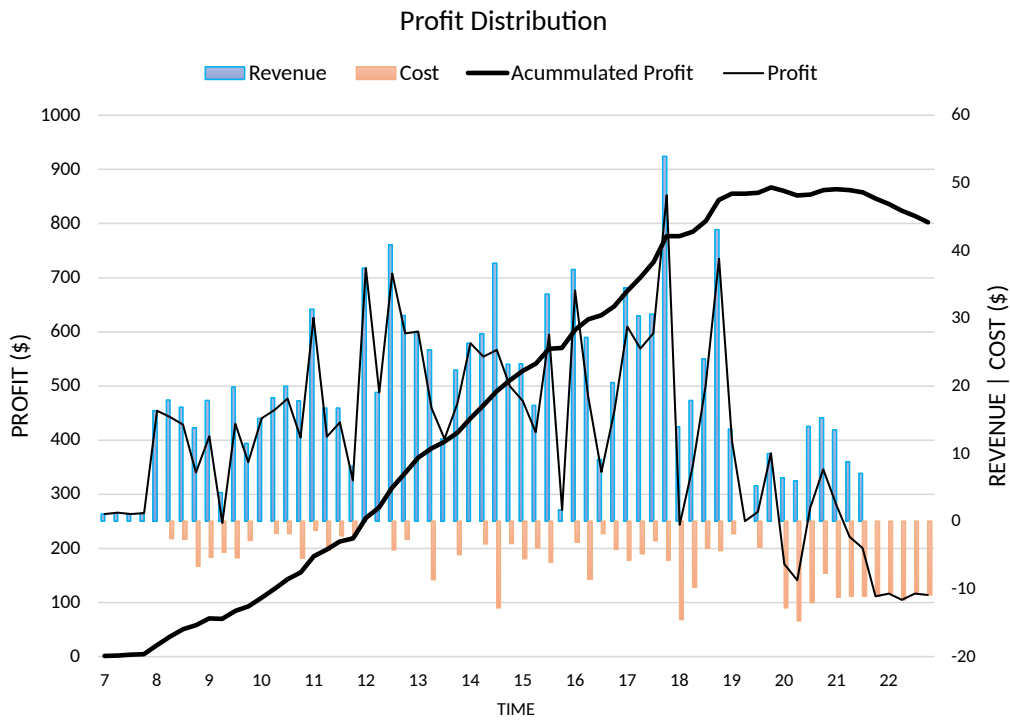


Figure 5.15: PV Energy use and Energy Price

### 5.3.5 EV Requests and Attendance

The BSS energy attendance decisions along the day can be seen for both Models 1 and 2 in Figs. 5.16 – 5.17, respectively. Since all requests have been accepted, these charts also describe the distribution of the 33 requests for Model 1 and 29 for Model 2 along the time. The yellow bars represent the minimum SOC required by the EV costumers, while the blue ones show the delivered energy above this minimum, which is not mandatory for the

BSS. A common pattern can be seen in both models, where all batteries above the minimum level are delivered until Hour 11, while the remaining are serviced at the minimum level. This profile shows the BSS ease in energy delivery during the first quarter of the day, since the energy is cheaper and each swapped battery can be quickly recharged. Further on, this profile can be directly related with the energy price profile and traffic curve interaction, since a lower frequency of swapping requests enables the BSS to charge the depleted batteries until the next request, while lower energy prices ensures a profitable process. In this sense, situations where there is a match between the energy peak price and many EV arrivals are tougher to be treated in the BSS operation.

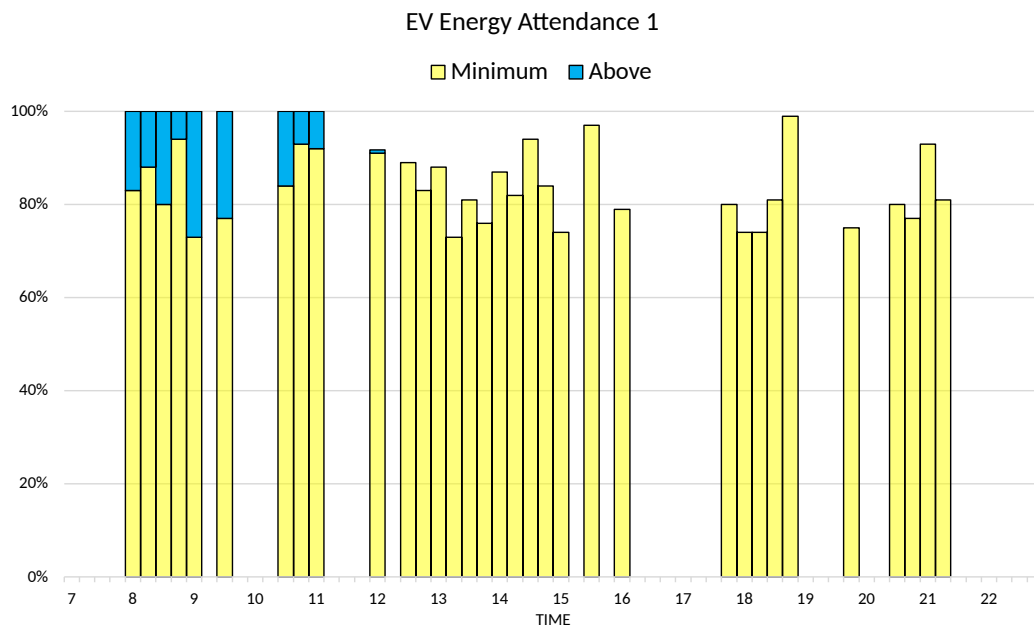


Figure 5.16: EV Energy Attendance for Model 1

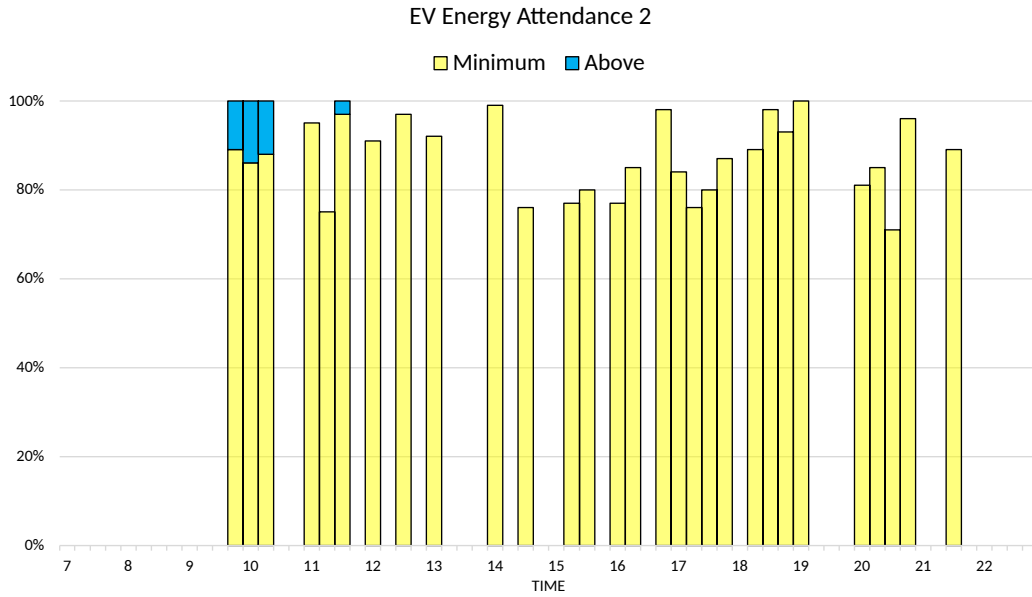


Figure 5.17: EV Energy Attendance for Model 2

### 5.3.6 BSS Economical Evaluation

Since this work argues towards BSS business model for the properly attendance of EVs, it is important to evaluate the use of this structure in several aspects for a global understanding. The previous analyses focused on the benefits by the BSS perspective, where is possible to see the financial feasibility of the operation even with a Service Level of 100%, especially due to the use of PV generation. In this sense, this section goes towards the costumers perspective, where a cost analysis is presented in order to see which structure better attends the costumers.

Figs. 5.18 – 5.19 summarizes the sold energy along the optimized case, illustrated by the orange bars, together with the spot price and the swapping price. For the sake of simplicity of costs comparison, it will be assumed that EV costumers would use fasting charge at the same time they would arrive at the BSS, therefore the energy price of their time arrival will be used for the charging cost reference. In this sense, fast charging users would operate the chart orange bars following the spot price, while BSS users operate with the constant swapping price, which is the 60th percentile of the day prices. Considering all costumers of the case, Table 5.3 summarizes the obtained values of this evaluation, thereby showing that the BSS offers a lower cost than the fast charging. This result can be directly associated to the high density of requests between Hours 17 and 19, which matches with the energy price's peak and tends to increase the charging costs. The BSS structure tends to mitigate this

problem with previously charged batteries, as well as the use of PV generation. Having a centralized structure that aims to charge at minimum cost is easier than transfer this job to several EV users that may not have the knowledge or time availability to do the same, especially treating the battery degradation properly.

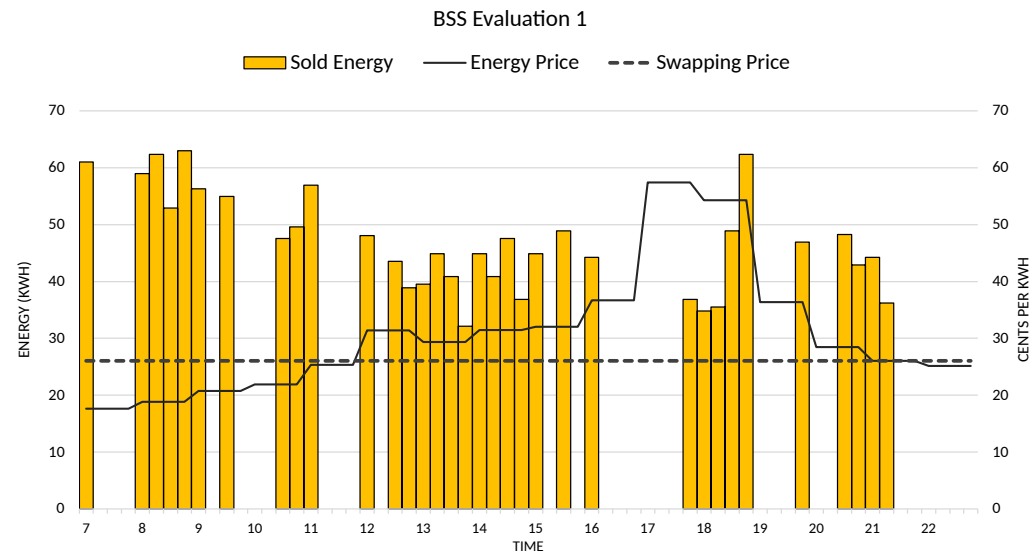


Figure 5.18: BSS Evaluation for Model 1

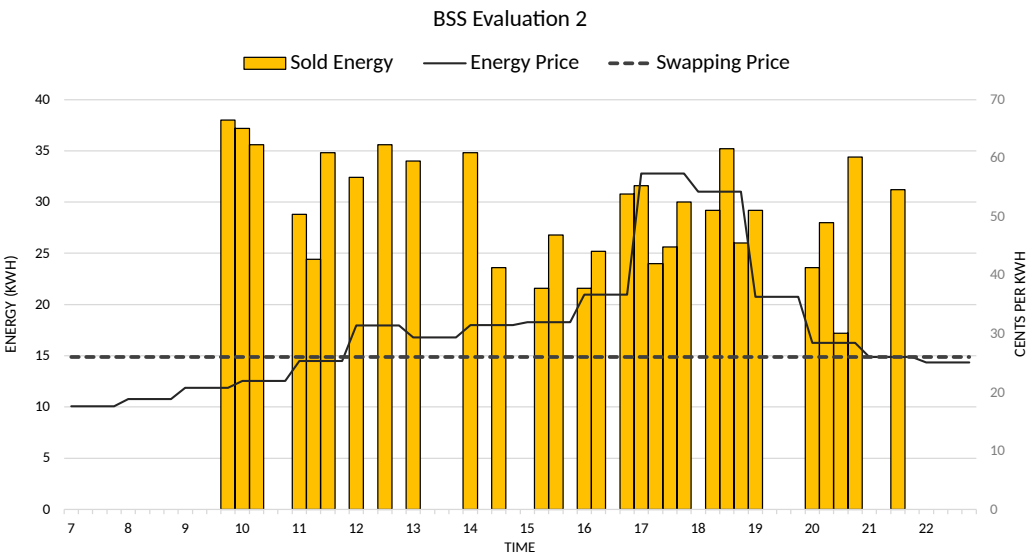


Figure 5.19: BSS Evaluation for Model 2

Table 5.3: BSS Economical Evaluation

Battery Model	1	2	Total
BSS Cost	\$415.72	\$221.44	\$637.16
Fast Charging	\$484.99	\$300.85	\$785.84

### 5.3.7 Sensitivities

This section explores sensitivities in the problem parameters to provide helpful insights with respect to the impact of a BSS sizing plan, PV capacity and number of available batteries. In this sense, this section evaluates the impacts of changes along the number of operating batteries, PV capacity and, at last, the impact of service level changes at the operation profit.

#### 5.3.7.1 Batteries Number

This section provides a sensitivity along the impacts of the number of batteries, exploring the benefits BSS operation expansion in terms of available batteries. Fig. 5.20 presents the battery number sensitivity, showing the impacts at the BSS profit and associated metrics FB and PA increasing each battery model by one unit. First of all, it is possible to notice a variable marginal profit gain along the possible numbers per type of battery that tends to decrease. Changing this number from four to five, it was achieved a gain of \$140.76, representing an increase of 17%, while the next gain had a drop to \$12.93, dropping this increase to only 1%. This behavior can be explained by a more loose operation as the batteries number increase, since the analyzed case study showed that four batteries per type are already sufficient for the operation, eventhough there will be profit increases with the use of more batteries, which must be planned accordingly with the investment cost.

Moreover, towards the metrics observed impacts, the increase in the percentage of full batteries delivery highlights a better swapping service, which together with the increase in power above limit use gives the conclusion that more batteries imply in a better use of cheap spot price moments. Overall, with a higher number of batteries, the BSS can make complete recharges in hours of cheaper price that will be worth even considering the cost increase in power above the limit  $L$ , which explains the metrics evolution in Fig. 5.20. As previously said, this decision must be planned together with the cost of acquiring new batteries for the station.

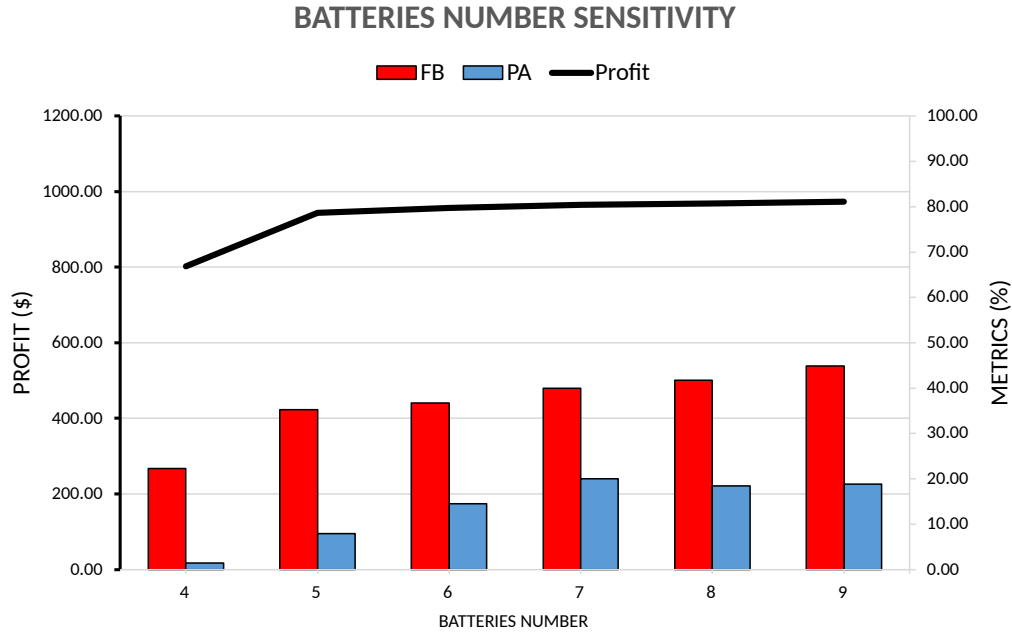


Figure 5.20: BSS Profit and Metrics Relation with Batteries Number

### 5.3.7.2

#### PV Capacity

This section explores the impact of the PV capacity in the BSS operation in terms of customer attendance and profit. The sensitivity results are presented in Fig. 5.21, where it is noticeable the high impact of PV capacity in the BSS profit, even showing losses in the case where there is no PV generation available. Overall, in the evaluated case, the profit gain was similar in all ranges of PV capacity, where it is observed a gain of \$446.00 for every 250kW of PV installed capacity added, which could be helpful for a BSS sizing plan. Moreover, the use of PV generation enables the swapping service at a fixed price for the whole day, thus making possible a lower price for the customers.

The metrics FB and PA are also shown in Fig. 5.21, since it is noticeable a constancy in the percentage of full batteries delivery, together with a decreasing in the power above limit used. These obtained results show that increased PV generation tends to reduce the amount of energy bought from the grid, decreasing the charging costs, while maintaining the same priority for both energy sale to grid and customers attendance.



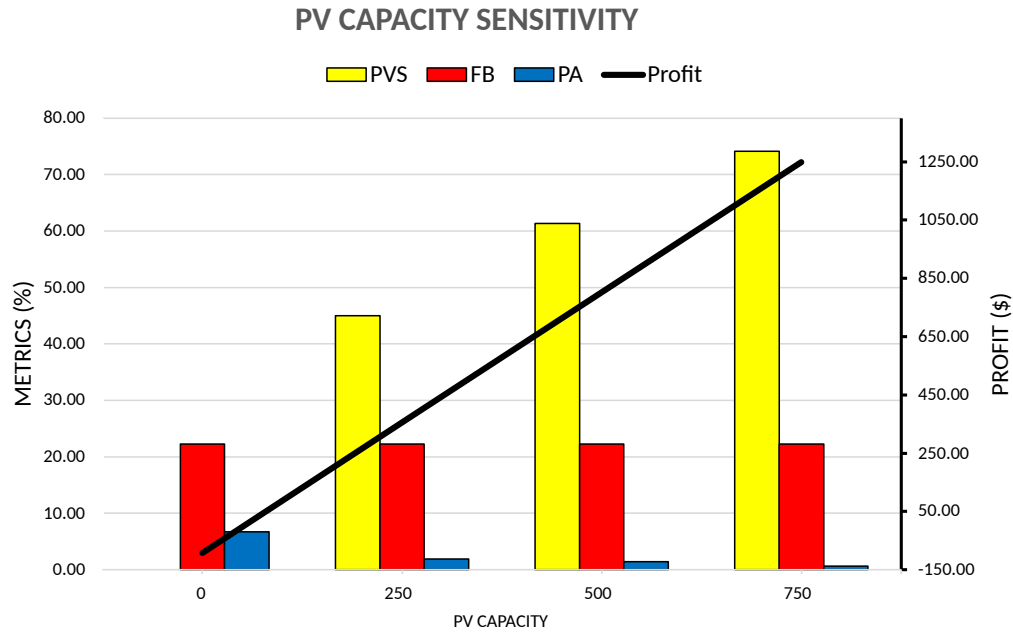


Figure 5.21: BSS Profit and Metrics Relation with PV Capacity

### 5.3.7.3 Service Level

This section provides a sensitivity along the impacts of the BSS costumers attendance in the profit and other BSS aspects. Following actual gas stations operations practice, where the fossil based fuels are storage at large amounts, the fuel price occasionally changes and often all costumers are fully supplied. A BSS business model, however, cannot follow the same behavior, since energy price is extremely volatile and there are limitations within actually energy storage capacity together with battery lifetime management difficulties. Fig. 5.22 shows the service level sensitivity results, where the star point highlights the service level around 40 and 50%, that achieves the best profit points considering the degradation as an immediate cost, evaluated at \$930.05 and \$928.86, respectively. Although this were the best points, it is noticeable by the chart's black curve that the profit differences are marginal until the Service Level of 90%, where there is a sudden drop until 100% value.

Overall, analyzing the profit marginal evolution, it is possible to conclude that higher service levels require the use of more expensive energy, thus reducing the BSS profit. Towards the degradation cost evolution, on the other hand, it is possible to notice the degradation almost linear increment, showing that higher charging rates are necessary to attend more swapping requests, therefore increasing battery degradation. All of these aspects must be considered by the business model plan, especially considering the drop

from Service Level 90%, where the profit disregarding the degradation cost is evaluated at \$956.36, which drops to \$802.76 at the 100% level, representing a drop of 19%. Ideally, the chosen business model should protect the BSS from eventual economical losses by planning the batteries rent payment based on a service level of reference.

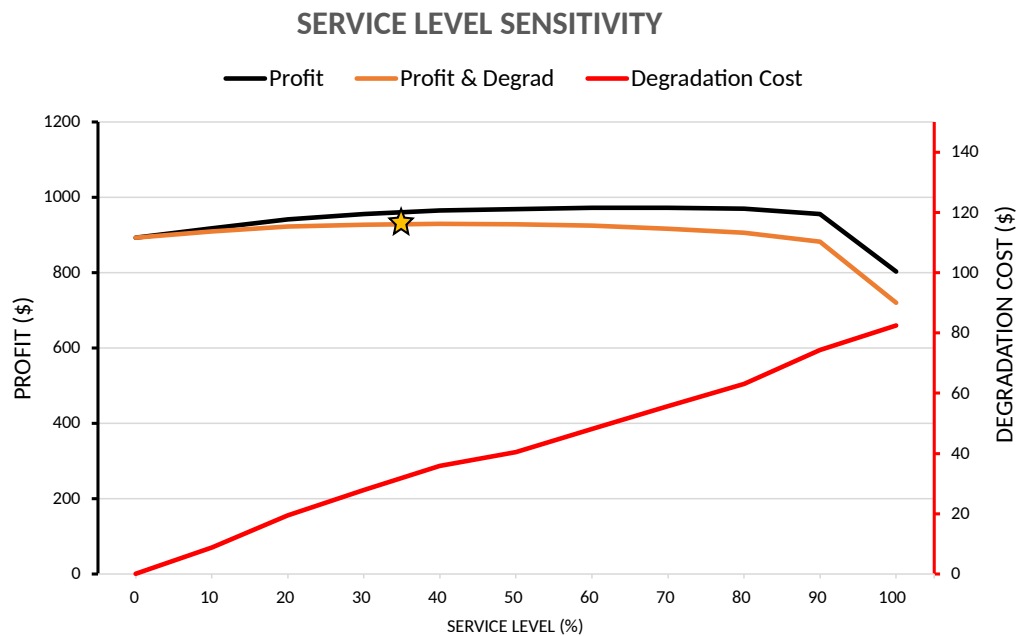


Figure 5.22: BSS Profit and Degradation relation with Service Level

## 6

### Conclusion

This work proposed a MILP problem to describe the BSS operation with PV power option considering multiple types of batteries. Battery degradation cost was considered by adapting an existing literature curve based exclusively on the battery charging rate, being treated with a piecewise linear function. Moreover, a charging control constraint was also developed in order to enhance the battery charging profile. Both proposed model extensions were evaluated and BSS metrics were developed in order to measure the station performance. Furthermore, four case studies were analysed based on realistic data from the US transportation and energy sectors. Numerical results brought insights over the BSS daily operation with a hourly energy price, presenting its PV power optimal use, grid charging over time, costumers attendance, and an expected daily profit of \$823.64 with a service level of 100% in the summer typical weekday analyzed. Sensitivities illustrated the impacts of batteries number, PV capacity and service level variation in the BSS profit and measurement metrics. Regarding the service level sensitivity, it was presented a considerable drop in the BSS profit when it aims over a service level of 90%, therefore bringing useful insights for BSS plannings and raising discussions about the BSS ideal business model.

Ongoing research includes the consideration of batteries SoH in the swapping process and second life batteries for operation support. Moreover, the consideration of a stochastic model development is in future research scope, where the uncertainty in EVs' time arrival and remaining energy would be considered. At last, the use of exact methods for model computational complexity enhancement, such as decompositions, are also being considered in future research.

## Bibliography

- [1] *Net Zero by 2050 – A Roadmap for the Global Energy Sector*. Tech. rep. International Energy Agency, Oct. 2021.
- [2] Aderson Campos Passos et al. “A Novel Framework to Define the Premium for Investment in Complementary Renewable Projects.” In: *2014 Power Systems Computation Conference*. Aug. 2014, pp. 1–7.
- [3] Alexandre Moreira, Goran Strbac, and Bruno Fanzeres. “An Ambiguity Averse Approach for Transmission Expansion Planning.” In: *2019 IEEE Milan PowerTech*. June 2019, pp. 1–6.
- [4] Arthur Brigatto and Bruno Fanzeres. “A Soft Robust Methodology to Devise Hedging Strategies in Renewable Energy Trading based on Electricity Options.” In: *Electric Power Systems Research* 207 (June 2022), p. 107852. DOI: 10.1016/j.epsr.2022.107852.
- [5] *Global EV Outlook 2021 – Accelerating Ambitions Despite the Pandemic*. Tech. rep. International Energy Agency, Apr. 2021.
- [6] Carlos Armenta-Deu and Erwan Cattin. “Real Driving Range in Electric Vehicles: Influence on Fuel Consumption and Carbon Emissions.” In: *World Electric Vehicle Journal* 12.4 (2021). ISSN: 2032-6653. DOI: 10.3390/wevj12040166.
- [7] Murat Yilmaz and Philip T. Krein. “Review of Battery Charger Topologies, Charging Power Levels, and Infrastructure for Plug-In Electric and Hybrid Vehicles.” In: *IEEE Transactions on Power Electronics* 28.5 (May 2013), pp. 2151–2169. DOI: 10.1109/TPEL.2012.2212917.
- [8] G. Joos, M. de Freige, and M. Dubois. “Design and Simulation of a Fast Charging Station for PHEV/EV Batteries.” In: *2010 IEEE Electrical Power & Energy Conference*. 2010, pp. 1–5. DOI: 10.1109/EPEC.2010.5697250.
- [9] Furkan Ahmad et al. “Battery Swapping Station for Electric Vehicles: Opportunities and Challenges.” In: *IET Smart Grid* 3.3 (June 2020), pp. 280–286. DOI: <https://doi.org/10.1049/iet-stg.2019.0059>.
- [10] Yu Zheng et al. “Electric Vehicle Battery Charging/Swap Stations in Distribution Systems: Comparison Study and Optimal Planning.” In: *IEEE Transactions on Power Systems* 29.1 (Jan. 2014), pp. 221–229. DOI: 10.1109/TPWRS.2013.2278852.

- [11] Yanni Liang and Xingping Zhang. “Battery Swap Pricing and Charging Strategy for Electric Taxis in China.” In: *Energy* 147 (Mar. 2018), pp. 561–577. ISSN: 0360-5442. DOI: <https://doi.org/10.1016/j.energy.2018.01.082>.
- [12] ACM. *Battery Swapping System*. Last accessed 24 May 2022. 2021. URL: <https://acm.city/battery-swapping-system/>.
- [13] Mingfei Ban et al. “Battery Swapping: An aggressive approach to transportation electrification.” In: *IEEE Electrification Magazine* 7.3 (2019), pp. 44–54. DOI: 10.1109/MELE.2019.2925762.
- [14] Adrian Konig et al. “An Overview of Parameter and Cost for Battery Electric Vehicles.” In: *World Electric Vehicle Journal* 12 (Feb. 2021), p. 21. DOI: 10.3390/wevj12010021.
- [15] Chang-Hua Zhang et al. “The adequacy model and analysis of swapping battery requirement for electric vehicles.” In: *2012 IEEE Power and Energy Society General Meeting*. 2012, pp. 1–5. DOI: 10.1109/PESGM.2012.6345365.
- [16] Pingping Xie et al. “A novel conceptual framework for electric vehicles participating in Automatic Generation Control: Station-to-grid.” In: *2012 China International Conference on Electricity Distribution*. 2012, pp. 1–5. DOI: 10.1109/CICED.2012.6508510.
- [17] Mushfiqu R. Sarker, Hrvoje Pandzic, and Miguel A. Ortega-Vazquez. “Electric vehicle battery swapping station: Business case and optimization model.” In: *2013 International Conference on Connected Vehicles and Expo (ICCVE)*. 2013, pp. 289–294. DOI: 10.1109/ICCVE.2013.6799808.
- [18] Ahmed A. Shalaby et al. “Optimal Day-ahead Operation for a PV-based Battery Swapping Station for Electric Vehicles.” In: *2021 6th International Symposium on Environment-Friendly Energies and Applications (EFEA)*. 2021, pp. 1–8. DOI: 10.1109/EFEA49713.2021.9406274.
- [19] Gurappa Battapothula, Chandrasekhar Yammani, and Sydulu Maheswarapu. “Multi-Objective Optimal Scheduling of Electric Vehicle batteries in Battery Swapping Station.” In: *2019 IEEE PES Innovative Smart Grid Technologies Europe (ISGT-Europe)*. 2019, pp. 1–5. DOI: 10.1109/ISGTEurope.2019.8905586.

- [20] Mohsen Mahoor, Zohreh S. Hosseini, and Amin Khodaei. “Least-cost operation of a battery swapping station with random customer requests.” In: *Energy* 172 (2019), pp. 913–921. ISSN: 0360-5442. DOI: <https://doi.org/10.1016/j.energy.2019.02.018>. URL: <https://www.sciencedirect.com/science/article/pii/S0360544219302075>.
- [21] Saeid Esmaili, Amjad Anvari-Moghaddam, and Shahram Jadid. “Optimal Operation Scheduling of a Microgrid Incorporating Battery Swapping Stations.” In: *IEEE Transactions on Power Systems* 34.6 (2019), pp. 5063–5072. DOI: 10.1109/TPWRS.2019.2923027.
- [22] Jiawei Feng et al. “Optimization of photovoltaic battery swapping station based on weather/traffic forecasts and speed variable charging.” In: *Applied Energy* 264 (2020), p. 114708. ISSN: 0306-2619. DOI: <https://doi.org/10.1016/j.apenergy.2020.114708>. URL: <https://www.sciencedirect.com/science/article/pii/S0306261920302208>.
- [23] Yang Gao et al. “Lithium-ion battery aging mechanisms and life model under different charging stresses.” In: *Journal of Power Sources* 356 (2017), pp. 103–114. ISSN: 0378-7753. DOI: <https://doi.org/10.1016/j.jpowsour.2017.04.084>. URL: <https://www.sciencedirect.com/science/article/pii/S0378775317305876>.
- [24] Ximeng Liu et al. “Securing the Internet-of-Things: Advances, challenges, future trends.” In: *Transactions on Emerging Telecommunications Technologies* 32 (May 2021). DOI: 10.1002/ett.4230.
- [25] Tanveer Ahmad et al. “Energetics Systems and artificial intelligence: Applications of industry 4.0.” In: *Energy Reports* 8 (2022), pp. 334–361. ISSN: 2352-4847. DOI: <https://doi.org/10.1016/j.egyr.2021.11.256>. URL: <https://www.sciencedirect.com/science/article/pii/S2352484721014037>.
- [26] Garth P. McCormick. “Computability of Global Solutions to Factorable Nonconvex Programs: Part I – Convex Underestimating Problems.” In: *Mathematical Programming* 10.1 (Dec. 1976), pp. 147–175.
- [27] Akshay Gupte et al. “Solving Mixed Integer Bilinear Problems using MILP Formulations.” In: *SIAM Journal on Optimization* 23.2 (2013), pp. 721–744.
- [28] Bruno Fanzeres, Shabbir Ahmed, and Alexandre Street. “Robust Strategic Bidding in Auction-Based Markets.” In: *European Journal of Operational Research* 272.3 (Feb. 2019), pp. 1158–1172.

- [29] Bruno Fanzeres, Alexandre Street, and David Pozo. “A Column-and-Constraint Generation Algorithm to Find Nash Equilibrium in Pool-Based Electricity Markets.” In: *Electric Power Systems Research* 189 (Dec. 2020), p. 106806.
- [30] Bolun Xu et al. “Modeling of Lithium-Ion Battery Degradation for Cell Life Assessment.” In: *IEEE Transactions on Smart Grid* 99 (June 2016), pp. 1–1. DOI: 10.1109/TSG.2016.2578950.
- [31] PJM. *Data Directory*. Last accessed 27 April 2022. 2021. URL: <https://www.pjm.com/>.
- [32] USDOT. *U.S. Department of Transportation: Our nation’s highways*. Last accessed 15 May 2022. 2011. URL: <https://www.fhwa.dot.gov/policyinformation/pubs/hf/pl11028/chapter4.cfm>.
- [33] PSR. *Time Series Lab*. Last accessed 20 May 2022. 2021. URL: <https://www.psr-inc.com/software/?current=p13880>.
- [34] Tesla. *Model 3*. Last accessed 10 May 2022. 2021. URL: <https://www.tesla.com/model3>.
- [35] Nissan. *Nissan Leaf*. Last accessed 10 May 2022. 2021. URL: <https://www.nissan.com.br/veiculos/modelos/leaf.html>.
- [36] Sofana Reka et al. “Analysis of Electric Vehicles with an Economic Perspective for the Future Electric Market.” In: *Future Internet* 14.6 (May 2022), pp. 1–17. URL: <https://ideas.repec.org/a/gam/jftint/v14y2022i6p172-d829466.html>.